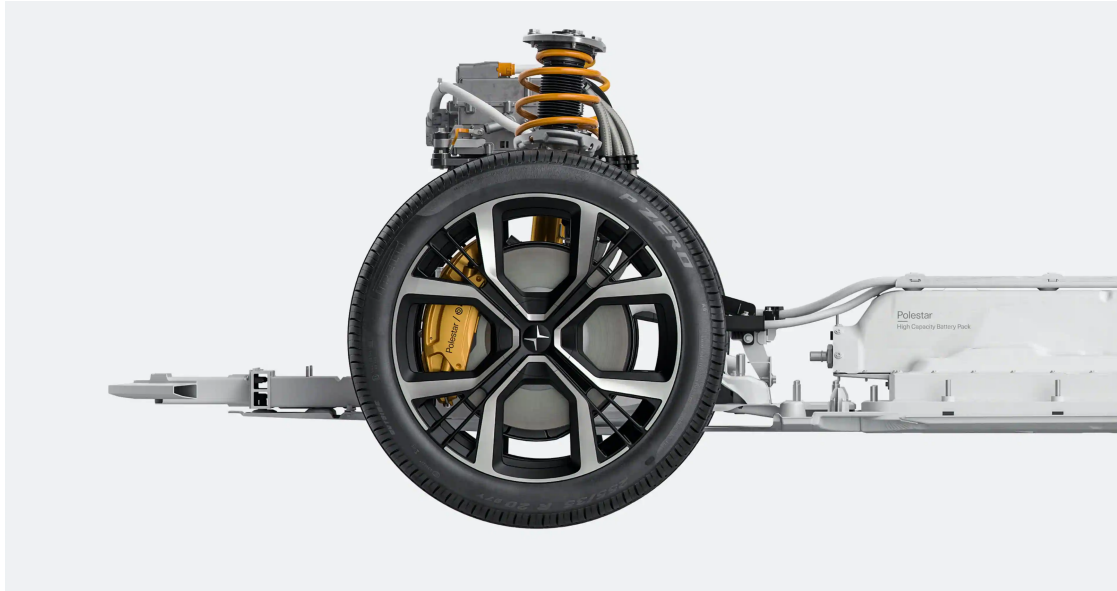




CHALMERS
UNIVERSITY OF TECHNOLOGY



Blending regenerative and friction ABS braking of an electrified vehicle

Feasibility analysis of incorporating a regenerative braking system with friction brakes during an ABS intervention, a numerical approach

Master's thesis in Systems, Control and Mechatronics (MPSYS)

ERNAD MEHINAGIC
LEJLA CRNIC

Blending regenerative and friction ABS braking of an electrified vehicle

Feasibility analysis of incorporating a regenerative braking system with friction brakes during an ABS intervention, a numerical approach

Master's thesis in Systems, Control and Mechatronics (MPSYS)

ERNAD MEHINAGIC
LEJLA CRNIC



CHALMERS
UNIVERSITY OF TECHNOLOGY

Department of Electrical Engineering
Division of Systems and Control
CHALMERS UNIVERSITY OF TECHNOLOGY
Gothenburg, Sweden 2020

Blending regenerative and friction ABS braking of an electrified vehicle

Feasibility analysis of incorporating a regenerative braking system with friction brakes during an ABS intervention, a numerical approach

ERNAD MEHINAGIC

LEJLA CRNIC

© ERNAD MEHINAGIC, LEJLA CRNIC 2020.

Supervisor: Staffan Johansson, Quintus Jalkler, Volvo Cars

Examiner: Nikolce Murgovski, Department of Electrical Engineering

Master's Thesis 2020: EENX30
Department of Electrical Engineering
Division of Systems and Control
Chalmers University of Technology
SE-412 96 Gothenburg
Telephone +46 31 772 1000

Cover: Layout of Polestar 2 front axle [1].

Typeset in L^AT_EX
Printed by Chalmers Reproservice
Gothenburg, Sweden 2020

Blending friction and regenerative ABS braking of an electrified vehicle
Feasibility analysis of incorporating a regenerative braking system with friction
brakes during an ABS intervention, a numerical approach
ERNAD MEHINAGIC, LEJLA CRNIC
Department of Electrical Engineering
Chalmers University of Technology

Abstract

Today, most vehicles are developed with the aim of having an optimal energy efficiency in order to reach sustainability goals. Major vehicle manufacturers share these values and are therefore trying to produce more efficient products by shifting to an electrified propulsion system. Regenerative braking is used in electrified vehicles in order to convert kinetic energy into electric energy using an electric motor (EM). The part of the brake energy that is not recovered using regenerative braking is covered by the friction brakes, thus could be considered as waste. Hence, it is beneficial if regenerative braking could be optimized. There are certain load cases for which regenerative braking could be used. One such load case is brake application that includes ABS intervention.

In this thesis an analysis was conducted, regarding the possibility to brake by merging a frictional and regenerative brake system during an ABS intervention. The integration of a regenerative brake system with an ABS, requires a blended brake control strategy. An optimal torque distribution between the operating brake systems is crucial, if one desires to perform optimal brake blending. The primary aim of this thesis was to develop a torque distribution controller that enhances the brake performance during straight road driving. Two torque distribution controllers were developed, one where maximal regenerative brake torque was applied and the other where a regulated amount of regenerative brake torque was used. Both strategies enhanced the braking performance by reducing the brake distance while still maintaining vehicle stability. Simulations show that a regulated amount of regenerative brake torque was more effective in terms of reducing brake distance, whereas by maximizing the regenerative brake torque gives a greater recuperation at the expense of reducing the brake distance.

The safety aspect during an ABS intervention is of highest priority, implying that reducing brake distance is of higher importance. The brake distance reduction was mainly possible due to the fast response time from the EM used during regenerative braking. The response time of the EM gave the braking a head start compared to the conventional system using only friction brakes. Comfortability constraints of the EM can be removed in order to further decrease the ramp-up time and give the EM an even greater advantage compared to the frictional brake system. The results gained from the analysis conducted in this report, indicates that this type of brake blending system gives the possibility to enhance brake performance.

Further research and development will enable brake blending during an ABS intervention in a real vehicle. The developed controllers still have room for improvement regarding performance and adaptability to altering driving scenarios, since the development was solely based on straight road driving. The current controllers have been substantiated using simulations only, in order to apply the controllers in a vehicle future steps of validation have been determined.

Keywords: Brake blending, Torque distribution, Regenerative braking, Friction brake, EM, ABS, Brake distance.

Acknowledgements

We would like to give our supervisor at Volvo Cars, Quintus Jalkler, a special thanks for helping us to acclimate to a new work environment and giving us guidance at the start of the thesis.

We would like to give our greatest thanks to our supervisor at Volvo Cars, Staffan Johansson, for being very invested in helping us achieving our goals in this thesis and for always providing us with valuable knowledge both professionally and in life. This thesis would not have been the same without your help.

We also want to give a big thank you to our examiner at Chalmers, Nikolce Murgovski, for giving us great feedback during our meetings and for guiding us forward through this process. We are very grateful for all the academic support you provided us with.

Lastly we want to give a great thank you to our families and friends, for supporting us throughout this thesis and the rest of our academic journey.

Ernad Mehinagic & Lejla Crnic, Gothenburg, 09 2020



Contents

List of Figures	xiii
List of Tables	xix
1 Introduction	1
1.1 Related work	1
1.2 Objective	2
1.3 Scope	2
1.4 Delimitations	3
2 Vehicle powertrain and braking system	5
2.1 Longitudinal vehicle dynamics	5
2.1.1 Single wheel model	7
2.1.2 Tire model (Friction estimator)	8
2.2 Brake systems used during brake blending	9
2.2.1 Friction brakes and braking by wire	9
2.2.2 Regenerative brake system	10
2.3 The electric motor and its properties	11
2.3.1 Electric power storage system	12
2.4 Anti-lock braking system	12
2.4.1 ABS-soft control strategy	12
2.4.2 Torque output of the ABS-soft model	13
2.5 Longitudinal dynamics during zero steering and constant heading	14
2.6 Brake blending during ABS	15
3 Methods	17
3.1 Preliminary analysis regarding the implementation of a torque distribution controller	17
3.2 General torque distribution approach	17
3.3 Approach II, Brake Blending with maximal usage of the electric motor	20
3.3.1 Switch implementations necessary for a beneficial torque distribution	21
3.4 Approach III, Brake Blending with a regulated usage of the electric motor	23
3.4.1 Calculation of constant electric motor torque	24
3.4.1.1 Achieving a desired brake torque request using an extreme-value function	24

3.4.1.2	Test on different road friction coefficients	25
3.4.1.3	Regulating brake torque request using a lookup table	25
3.4.1.4	Consideration of electric motor limitations	25
3.4.1.5	Torque conversion using a gear ratio	26
3.5	Simulation tools used for model-construction and result provision . .	26
4	Results & Discussion	27
4.1	Approach II, Brake Blending with maximal usage of the electric motor	28
4.1.1	Comparison of brake torque when using brake blending and when not using brake blending	28
4.1.2	Comparison of slip when using brake blending and when not using brake blending	30
4.1.3	Deceleration when using brake blending and when not using brake blending	31
4.1.4	Comparison of velocity when using brake blending and when not using brake blending	31
4.1.5	Comparing brake distance when using brake blending and when not using brake blending	32
4.2	Approach III, Brake Blending with a regulated usage of the electric motor	34
4.2.1	Comparison of brake torque when using brake blending and when not using brake blending	34
4.2.2	Comparison of slip when using brake blending and when not using brake blending	36
4.2.3	Comparison of deceleration when using brake blending and when not using brake blending	37
4.2.4	Comparison of velocity when using brake blending and when not using brake blending	37
4.2.5	Comparing brake distance when using brake blending and when not using brake blending	38
4.3	Design of experiments	40
5	Conclusion	43
6	Recommendation for future work	45

List of Figures

1.3.1	Flowchart representation of the work flow in this thesis. The grey blocks are each one of the main parts of the work flow. The text in white describes how the work in each segment was conducted. The coloured circles describe how to transition into next state of the work flow.	3
2.0.1	Picture of the Polestar 2.	5
2.1.1	Four wheel model representation.	6
2.1.2	Single wheel dynamics representation	7
2.1.3	Plot of road friction coefficient curve, where the x-axis is the slip ratio λ in %, which ranges from values between 0% to 100%. The y-axis is the estimated road friction coefficient, μ_i , which has a maximum value of around 0.9 at a slip ratio of approximately 20%.	9
2.2.1	The figure represents a part of the friction brake system. In the figure the brake disc and the brake caliper are visible.	9
2.2.2	The hydraulic brake by wire brake system in Polestar 2.	10
2.3.1	Plot of the torque output from the electric motor, which has a maximum value of 330 Nm.	11
2.4.1	This figure is visualization of how M_{ABS_i} is divided between each frictional brake for each wheel, during a brake application which includes ABS intervention. The curve is plotted after 10s since the ABS intervention is initiated at 12s and terminated when the vehicle has stopped at approximately 15s.	13
2.4.2	A representation of the pulsations (similar pulsations in all wheels) in the demanded torque for the front left wheel , caused by ABS-soft. The frequency is determined by how often the pressure has to be maintained, reduced or released in order to perform slip/wheel-control. The pulsations are presented at a randomly selected time interval from the time period where these pulsations occur.	14
2.6.1	Control block diagram of the brake-blending system	15

3.2.1 The signal-path is from top to bottom. M_{ABS_i} , is dependent on variables such as ω_i , λ_i , R and M_{dem_i} . The ABS-soft model calculates the requested torque M_{ABS_i} and the EM provides the brake torque $\frac{M_{EM_j}}{2}$ based on the brake torque request M_{EMreq_j} . M_{EM_j} is then subtracted from M_{ABS_i} and the remaining part of M_{ABS_i} is sent to the frictional brake system as M_{fric_i} . The frictional brake system then sends M_{fric_i} and $\frac{M_{EM_j}}{2}$ is added to provide with M_{wheel_i} 18

3.2.2 Schematic view of complete brake system, including a visual representation of the brake torque distribution. 19

3.3.1 Flowchart representation of Approach II. The signal-path is from top to bottom. The torque request from ABS-soft, M_{ABS_i} , is dependent on variables such as ω_i , λ_i , R and M_{dem_i} . The ABS-soft model calculates the requested torque M_{ABS_i} and the EM provides the brake torque $\frac{M_{EM_j}}{2}$ based on the brake torque request M_{EMreq_j} . M_{EM_j} is then subtracted from M_{ABS_i} and the remaining part of M_{ABS_i} is sent to the frictional brake system as M_{fric_i} . The frictional brake system then sends M_{fric_i} and $\frac{M_{EM_j}}{2}$ is added to provide with M_{wheel_i} 21

3.3.2 This figure visualizes the switch-logic, which starts from left by sending a constant value of 0 and the torque produced by the EM, M_{EM_j} , to the block to its right, which sends the maximal value of the two inputs. 22

3.3.3 A visualization of the switch-logic constructed with the cause of preventing negative M_{fric_i} to be sent to the friction brakes. The logic starts with the left side, where a constant value of zero and the difference between M_{ABS_i} and M_{EM_j} , are used as inputs to the max block. The max block then gives a positive value M_{fric_i} as an output. 22

3.3.4 This figure is a visual representation of the "system activator", where the three inputs to the left are, M_{EMreq_j} (u_1), Brake Pressure (BP), (u_2) and a constant value of zero (u_3). These are the inputs to the switch following to the right, where it gives an output of M_{EMreq_j} if BP is larger than 0, else a constant value of 0 is the output. 22

3.4.1 The figure is a flowchart visualization of the torque distribution strategy developed for Approach III. The flow starts from the top, divided in two pathways, one were the M_{ABS_i} is sent directly to the distribution block and the other were the constant M_{EMreq_j} is calculated first and then sent to the EM. The EM then sends a constant brake torque $\frac{M_{EM_j}}{2}$, which is removed from M_{ABS_i} in order to send the rest, M_{fric_i} , to the friction brakes. The frictional brake system then returns M_{fric_i} and together with $\frac{M_{EM_j}}{2}$ provides M_{wheel_i} 23

3.4.2 The figure is a representation of how the extreme-value function is choosing M_{lookup_j} (red line) right before the oscillations seen in the demanded torque(blue curve). 24

-
- 3.4.3 A flowchart representation of the EM limitations is presented inside the red square. The flow goes from top to bottom, starting with the road friction coefficient as an input to a lookup table, which then has the corresponding constant brake torque, referred to as M_{lookup_j} , as an output. M_{lookup_j} is then checked in the following block, if it can be realized or if it is limited by the EM. Depending on if it passes the condition or not, it can take two different pathways. Both of the paths goes through the Torque converter where *gear* is removed and leaves M_{EMreq_j} , which is being sent directly to the EM. 25
- 4.1.1 The figure is a representation of how Approach II performs during Test Case 1 compared to Approach I, where each subplot represents one of the wheels. The curve is plotted after 10s since the brake application starts at time $t \geq 12$ s and is terminated when the vehicle has stopped at approximately 15s. The one second pause interval starts at $t \approx 11$ s and ends at $t \approx 12$ s, the brake application therefore starts at time $t \geq 12$ s. 28
- 4.1.2 The figure is a representation of how Approach II performs during Test Case 2 compared to Approach I, where each subplot represents one of the wheels. The curve is plotted after 10s as the brake application starts at time $t \geq 11$ s and is terminated when the vehicle has stopped at approximately 14.5s. 29
- 4.1.3 A visual representation of the slip comparison between Approach I and Approach II, for Test Case 1 (left plot) and Test Case 2 (right plot). Both plots are a representation of the front left wheel. The curves are plotted after 10s since the brake application starts at time $t \geq 12$ s for Test Case 1 and $t \geq 11$ s for Test Case 2. The one second pause interval for Test Case 1 starts at $t \approx 11$ s and ends at $t \approx 12$ s, when the pause interval is completed the brake applications is initiated. The brake application for Test Case 1 is terminated when the vehicle has stopped at approximately 15s and for Test Case 2 at approximately 14s. 30
- 4.1.4 The figure is a representation of the resulting vehicle deceleration comparison, between Approach I and Approach II, during Test Case 1 (left plot) and Test Case 2 (right plot). The vehicle did not start to accelerate (positive valued curve) until $t \geq 2$ s for Test Case 1 and 2. The curves are plotted after 10s since the brake applications starts at time $t \geq 12$ s for Test Case 1 and $t \geq 11$ s for Test Case 2. The one second pause interval for Test Case 1 starts at $t \approx 11$ s and ends at $t \approx 12$ s, when the pause interval is completed the brake application is initiated. The brake application for Test Case 1 is terminated when the vehicle has stopped at approximately 15s and for Test Case 2 at approximately 14s. 31

4.1.5	The figure is a representation of the resulting vehicle velocity when using Approach I and II, during Test Case 1 (left plot) and Test Case 2 (right plot). The vehicle does not start to accelerate until $t \geq 2$ s for Test Case 1 and 2. For Test Case 1 the one second pause interval starts at $t \approx 11$ s and ends at $t \approx 12$ s , when the pause interval is completed the brake applications starts at time $t \geq 12$ s . In Test Case 2 the brake application is initiated at $t \geq 11$ s . The brake application initiation is marked in both plots with a grey square, where it can be seen that velocity between Approach I and II differs for both cases.	32
4.1.6	The figure is a representation of the resulting vehicle brake distance when using Approach I and II, during Test Case 1 (left plot) and Test Case 2 (right plot). The brake application starts at time $t \geq 12$ s for Test Case 1. In Test Case 2 the brake application is initiated at $t \geq 11$ s	33
4.1.7	The figure is a representation of the brake distance difference between Approach I and Approach II for Test Case 1 and 2. The x-axis represents the time that the car is braking and the y-axis represents how big the difference is between the brake distance for Approach I and Approach II.	33
4.2.1	The figure is a representation of how Approach III performs during Test Case 1 compared to Approach I, where each subplot represents one of the wheels. The one second pause interval is starting at $t \approx 11$ s and ending at $t \approx 12$ s , when the pause interval is completed the brake applications starts at time $t \geq 12$ s	34
4.2.2	The figure is a representation of how Approach III performs during Test Case 2 compared to Approach I, where each subplot represents one of the wheels. The brake applications starts at time $t \approx 11$ s	35
4.2.3	A visual representation of the slip comparison between Approach I and Approach III, for Test Case 1 (left plot) and Test Case 2 (right plot). Both plots are a representation of the front left wheel. The brake application ends at approximately 15.5s for Test Case 1 and around 14.5s for Test Case 2.	36
4.2.4	The figure is a representation of the resulting vehicle deceleration comparison, between Approach I and Approach III, during Test Case 1 (left plot) and Test Case 2 (right plot). The vehicle does not start to accelerate (positive valued curve) until $t \geq 2$ s for Test Case 1 and 2. For Test Case 1 the one second pause interval is starts at $t \approx 11$ s and ends at $t \approx 12$ s, when the pause interval is completed the brake application starts at time $t \geq 12$ s. In Test Case 2 the brake application is initiated at $t \geq 11$ s. For both Test Case 1 and 2 a positive spike at 1g-force is visible at around 15 s , meaning that the brake application is terminated and the vehicle is no longer in motion (this is not relevant and thus not considered in the results).	37

4.2.5	The figure is a representation of the resulting vehicle velocity when using Approach I and III, during Test Case 1 (left plot) and Test Case 2 (right plot). The vehicle does not start to accelerate until $t \geq 2$ s for Test Case 1 and 2. For Test Case 1 the one second pause interval starts at $t \approx 11$ s and ends at $t \approx 12$ s, when the pause interval is completed the brake applications starts at time $t \geq 12$ s. In Test Case 2 the brake application is initiated at $t \geq 11$ s. The brake application initiation is marked in both plots with a grey square, where it can be seen that velocity between Approach I and III differs for both cases.	38
4.2.6	The figure is a representation of the resulting vehicle braking distance when using Approach I and III, during Test Case 1 (left plot) and Test Case 2 (right plot). The brake application starts at time $t \geq 12$ s for Test Case 1. In Test Case 2 the brake application is initiated at $t \geq 11$ s.	39
4.2.7	The figure is a representation of the brake distance difference between Approach I and Approach III for Test Case 1 and 2. The x-axis represents the time that the car is braking and the y-axis represents how big the difference is between the brake distance for Approach I and Approach III.	39
4.3.1	The figure represents a DOE where the different brake distance results for each Approach is visible.	40
4.3.2	The Figure represents what happens with one of the wheels when Approach II performs poorly on a road friction coefficient of 0.5. It can be seen from the red EM curve how the electric motor is trying to pulsate but has a slow ramp-up, since the ramp-up time is limited by a comfort constraint.	41
4.3.3	The Figure represents what happens with one of the wheels when Approach III performs well on low road friction coefficient. It can be observed that the pulsations are handled by the friction brakes and not by the EM as they are in Approach II.	41

List of Tables

- 2.1 A table with values of constants A (peak value of the road friction), B (road friction curve shape) and C (road friction curve difference between the maximum value and the value at $\lambda_i = 1$). The values of these constants are determined by the condition of having dry asphalt. 8

1

Introduction

Today, the majority of vehicles are developed with the aim of having an optimal energy efficiency in order to reach sustainability goals. Major vehicle manufacturers share these values and are therefore trying to produce more efficient products by shifting to electrified propulsion systems [2]. An example of electrified propulsion is Battery Electric Vehicles (BEVs), which is a technology that is looked upon as a promising solution to more sustainable transportation, as it has the potential to replace vehicles that are powered by fossil fuels [2]. The electrified powertrain system enables new functions and possibilities, alongside being more efficient than traditional vehicles, they allow for the recuperation of mechanical energy into electrical energy also known as regenerative braking [3, 4].

Regenerative braking is used in cars in order to convert kinetic energy into electric energy using an electric motor and a battery. Electric vehicles often use regenerative braking combined with friction brakes, which is also known as brake blending. Research and use of brake blending is focused on conventional deceleration levels [5]. However, brake blending is not utilized in emergency braking scenarios, when the Anti-lock Braking System (ABS) is activated. As mentioned in [5, 6], when ABS is activated the regenerative braking torque will be removed, which means that only the friction brakes will operate, to prevent possible wheel lock and stability issues. This is due to the fact that poorly handled regenerative braking can result in vehicle instability, reduce handling capability and decrease braking performance [7]. Another issue with regenerative braking is that limited electric motor power will cause difficulties at a higher deceleration rate, as more power is required to slow down the vehicle down than is available [8].

1.1 Related work

Earlier research [9, 10, 11, 12] has focused on determining the possibilities of integrating ABS with regenerative braking, without decreasing brake performance. The researchers in [9] have shown that it is possible to integrate and recover a significant amount of braking energy. However their research has been performed on a bicycle wheel which leaves the question of how realistic the results are for a car wheel. This question has been addressed by researchers in [10] which have tested their regenerative braking based ABS controller, in both simulation and on a real

vehicle. Their results show an improved energy recovery during ABS-situations by 60% in simulation and 40% in real vehicle test [10].

Similar research has been made in [11, 12]. Brake blending control, where regenerative braking is merged with a frictional brake system, has been studied in order to attempt to understand the capabilities of the regenerative braking system. The energy recovery limits have been investigated along with how these limits can affect the stability or maneuverability of the vehicle at hand. Electric motors were used for a certain fraction of the requested brake torque, while the remaining part was handled by the friction brakes. These simulations were performed on a hybrid vehicle with one electric motor on the rear axle. There were two proposed torque distribution control strategies, where the results from both imply that rear axle regenerative braking can be effective [11, 12].

As can be seen from above, there were several studies that suggest that brake blending is possible and beneficial and that there are several approaches to the problem. Therefore the main challenges lie with the smooth interaction between friction and regenerative brakes, along with proper torque distribution in brake blending systems, for these systems to be feasible.

1.2 Objective

The objective of this thesis is to develop a torque distribution controller, that splits brake torque between a regenerative and frictional braking system, during ABS intervention. There are two main research questions that need to be answered in order to be able to achieve the project goals:

1. How will the torque split affect the brake distance?
2. How much regenerative braking can be effectively applied?

1.3 Scope

The project began with finding a suitable controller for a car that accelerates to 130 km/h and proceeds to decelerate as quickly as possible. This scenario can cause wheel lock and loss of traction which activates the ABS function. The main focus of the project was to develop a control model that will make an optimal torque distribution between friction brakes and regenerative braking while ABS is active.

The controller could not be developed without necessary preparations. Figure 1.3.1 is a visual representation of the necessary steps that were taken in order to develop a torque distribution controller.

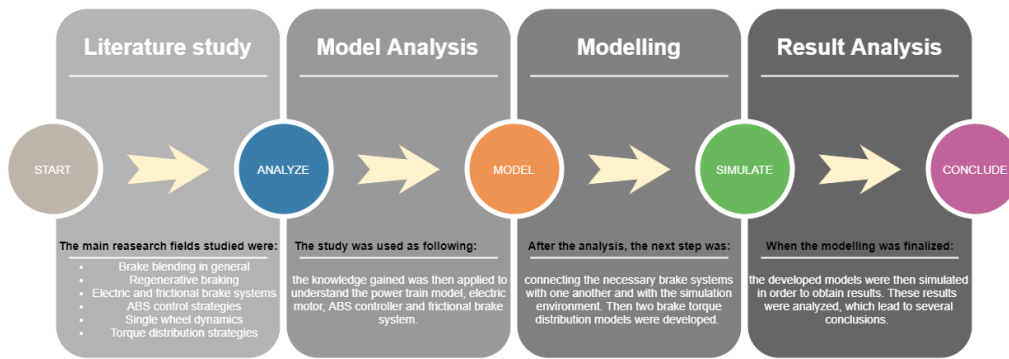


Figure 1.3.1: Flowchart representation of the work flow in this thesis. The grey blocks are each one of the main parts of the work flow. The text in white describes how the work in each segment was conducted. The coloured circles describe how to transition into next state of the work flow.

1.4 Delimitations

The following points are the delimitations set in this project

- It was assumed that the car drives on a straight road and that the steering will always keep the car in a straight line, meaning no lateral or horizontal displacements were considered.
- The road friction coefficient was selected relatively low in order to easily trigger ABS and was altered to see how the control models perform on different surfaces, however only two were used for the controller evaluation.
- The battery state of charge was considered as constant, meaning that battery limitations are not considered. Temperature influence was not considered, e.g that from high battery temperature that can affect the possibility of regeneration or the effects of the electric motor during high operating temperatures.
- Parameters such as the operating efficiency and the conversion efficiency for converting into regenerative braking will not be considered.
- The simulations are performed solely on one type of vehicle, the Polestar 2 and the brake blending is tested with one ABS model, ABS-Soft provided by IPG [13].

2

Vehicle powertrain and braking system

The vehicle used in this study is the premium all-electric 5-door all-wheel drive (AWD) Polestar 2. This car was developed based on Volvo Car Group's adaptable Compact Modular Architecture platform (CMA)[1]. The Polestar 2 falls into the category of a battery electric vehicle (BEV). The body-shape of the Polestar 2 is a "fastback" shape, very similar to a sedan body-shape, except that the rear window and boot door open as one unit[1].



Figure 2.0.1: Picture of the Polestar 2.

2.1 Longitudinal vehicle dynamics

This aim of the section is to provide the reader with some basics in longitudinal dynamics, in order to give a better understanding how certain forces are connected. The dynamics are primarily presented for the entire vehicle (4 wheels) and is then

narrowed down to single wheel dynamics. The ABS controller used in this project is based on single wheel dynamics and the torque distribution controller will work accordingly.

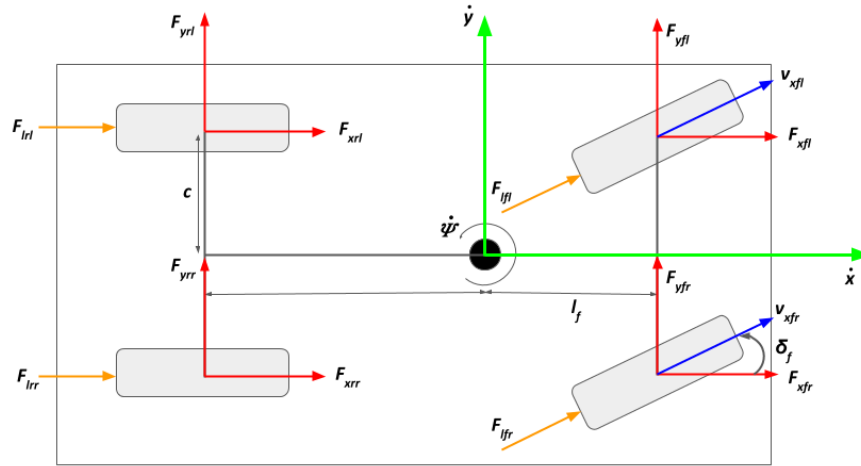


Figure 2.1.1: Four wheel model representation.

This project has only considered longitudinal movements and no lateral displacements. The longitudinal forces acting on the vehicle are expressed in the equations below and are also visible in Figure 2.1.1. Even though no turning motions are considered, the vehicle yaw rate ($\dot{\psi}$) and the turning angle rate of the wheel ($\dot{\delta}$) are represented in the figure and in equations. This is done to show how longitudinal forces are affected by lateral movements.

With the help of Newtons second law a force balance along the longitudinal axis can be represented as

$$m\ddot{x} = m\dot{y}\dot{\psi} + \sum F_{x_i}, \quad i = \{fl, fr, rl, rr\} \quad (2.1)$$

where m is the vehicle mass, \ddot{x} is the longitudinal acceleration, F_{x_i} is the tire force in vehicle body frame. The subscript i indicates what wheel is referred to, where fl stands for front left wheel, fr front right wheel, rl rear left wheel and rr rear right wheel.

The tire force mapping from wheel to vehicle body frame and can be represented as

$$F_{x_i} = \mu_i(\lambda_i)F_{N_i} \cos(\delta_j), \quad j = \{f, r\} \quad (2.2)$$

where λ_i is longitudinal slip ratio, μ_i is road friction coefficient and F_{N_i} is the normal force. Subscript j is indicating which axle a variable belongs to, and it works as follows, f (front) and r (rear). The longitudinal wheel velocity, v_{l_i} , defined in the tire frame, is expressed as

$$v_{l_i} = v_{x_i} \cos(\delta_j) \quad (2.3)$$

where v_{x_i} is the longitudinal wheel speed in the vehicle frame. This speed is related to the vehicle speed,

$$v_{x_{fr}} = \dot{x} + c\psi \quad (2.4)$$

$$v_{x_{fl}} = \dot{x} - c\psi \quad (2.5)$$

$$v_{x_{rr}} = \dot{x} + c\psi \quad (2.6)$$

$$v_{x_{rl}} = \dot{x} - c\psi \quad (2.7)$$

where c is the length between the center of the wheel and the center of the respective axle. Representation of signals associated to each wheel can be seen in equations (2.4) to (2.7).

2.1.1 Single wheel model

Figure 2.1.2 is a visual representation of the single wheel model, used in order to provide the reader with a clearer view of the single wheel dynamics.

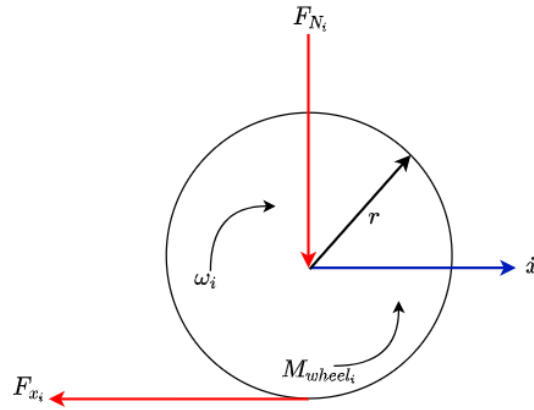


Figure 2.1.2: Single wheel dynamics representation

In this project the vehicle is assumed to have a straight motion, meaning that no lateral forces are considered. This will give the system one degree of freedom (DOF) on each wheel. The model is describing the elementary dynamic properties of the system [14], and its equation of motion is described as

$$J_i \dot{\omega}_i = -F_{x_i} R + M_{wheel_i} - b_d \omega_i. \quad (2.8)$$

In equation (2.8), M_{wheel_i} is the brake torque provided for each wheel, ω_i is the angular speed of the wheel, J_i is the wheel rotational moment of inertia, R is the wheel radius, b_d is a damping factor.

Equation (2.9) is a representation of how the two different brake systems are providing with the brake torque applied on each wheel.

$$M_{wheel_i} = M_{fric_i} + \frac{M_{EM_j}}{2} \quad (2.9)$$

Here, $M_{fric_i} \leq 0$ is the braking torque provided by the friction brakes for each wheel and M_{EM_j} is the torque provided by the EM on axle j . Equation (2.10) is then a representation of each wheel.

$$J_i \dot{\omega}_i = \begin{cases} J_{fr} \dot{\omega}_{fr} = -F_{x_{fr}} R + M_{fric_{fr}} + \frac{M_{EM_f}}{2} - b_d \omega_{fr}, & i = fr \\ J_{fl} \dot{\omega}_{fl} = -F_{x_{fl}} R + M_{fric_{fl}} + \frac{M_{EM_f}}{2} - b_d \omega_{fl}, & i = fl \\ J_{rr} \dot{\omega}_{rr} = -F_{x_{rr}} R + M_{fric_{rr}} + \frac{M_{EM_r}}{2} - b_d \omega_{rr}, & i = rr \\ J_{rl} \dot{\omega}_{rl} = -F_{x_{rl}} R + M_{fric_{rl}} + \frac{M_{EM_r}}{2} - b_d \omega_{rl}, & i = rl \end{cases} \quad (2.10)$$

The EM torque is equally distributed between the left and right wheel. During braking, when the longitudinal wheel speed is greater than or equal to its angular speed, i.e. $v_{l_i} \geq R\omega_i$, the wheel may start to slip. Then, the longitudinal wheel slip λ_i is derived as

$$\lambda_i = \frac{R\omega_i - v_{l_i}}{v_{l_i}}, \quad \text{if } v_{l_i} \geq R\omega_i, \quad v_{l_i} \neq 0. \quad (2.11)$$

2.1.2 Tire model (Friction estimator)

In this thesis, the Burckhardt model will be used, as it is optimized for analytical determinations while maintaining accuracy within the delimitations set for the project while estimating the road friction coefficient. Hence, the longitudinal friction coefficient estimator is as follows

$$\mu_i(\lambda_i) = A(1 - e^{-B\lambda_i} - C\lambda_i) \quad (2.12)$$

A (peak value of the road friction), B (road friction curve shape) and C (road friction curve difference between the maximum value and the value at $\lambda_i = 1$) are constants that changes depending on the road surface. Dry asphalt is the condition which will be used, where the values of each coefficient can be seen in Table 2.1[15].

<i>Estimator coefficients</i>			
<i>Condition</i>	<i>A</i>	<i>B</i>	<i>C</i>
Dry asphalt	1.029	17.16	0.523

Table 2.1: A table with values of constants A (peak value of the road friction), B (road friction curve shape) and C (road friction curve difference between the maximum value and the value at $\lambda_i = 1$). The values of these constants are determined by the condition of having dry asphalt.

The slip ratio-friction coefficient curve has been plotted with the help of Matlab and is visible below in Figure 2.1.3.

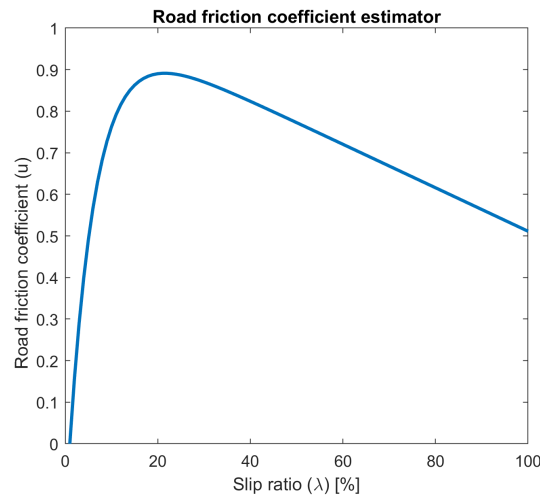


Figure 2.1.3: Plot of road friction coefficient curve, where the x-axis is the slip ratio λ in %, which ranges from values between 0% to 100%. The y-axis is the estimated road friction coefficient, μ_i , which has a maximum value of around 0.9 at a slip ratio of approximately 20%.

2.2 Brake systems used during brake blending

The entire brake system consists of two types of systems, a frictional brake system and a regenerative brake system. The frictional brake system is not modelled within this work, since it is provided by IPG's CarMaker. CarMaker, along with Simulink is used to model the torque distribution controller. The powertrain model is provided by Volvo and the ABS model is provided by IPG. The goal is to allocate this brake torque request between the two different brake systems.

2.2.1 Friction brakes and braking by wire

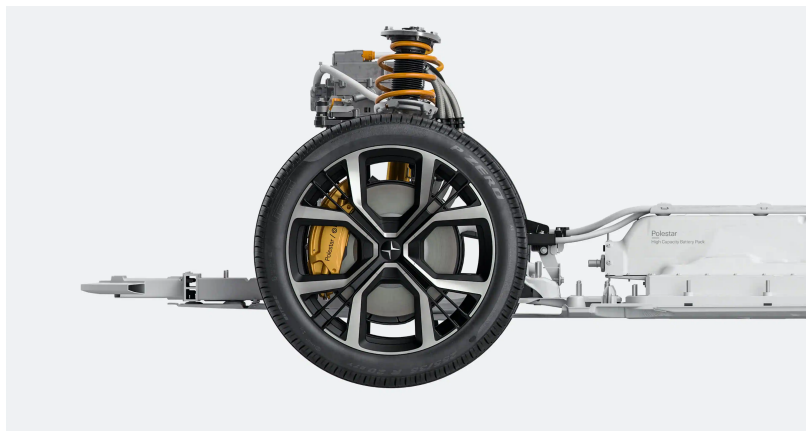


Figure 2.2.1: The figure represents a part of the friction brake system. In the figure the brake disc and the brake caliper are visible.

Friction brakes are mechanical devices which are used to decelerate the vehicle by converting hydraulic pressure to clamp force, thus creating brake torque. Friction brakes are also known as hydraulic brakes since they use fluid to create a brake pressure. The hydraulic brakes are divided in two categories, brake by wire or full hydraulic. Full hydraulic implies brake system in the car uses brake fluid to mechanically brake the wheels, while brake by wire controls the hydraulic pressure at the wheel using electrical means.

The brake by wire system is mechanically decoupling the brake pedal from the hydraulic brake system, which is increasing the flexibility of the brake torque modulation. Brake by wire fits well with vehicles that use frictional brakes and regenerative braking system in cooperation. The brake by wire system can achieve ideal brake torque distribution by modulating the brake torques between rear and front axle. The brake torque allocation has to be taken into consideration when trying to achieve an effective regenerative system and assure that no wheel lock occurs [5].

2.2.2 Regenerative brake system

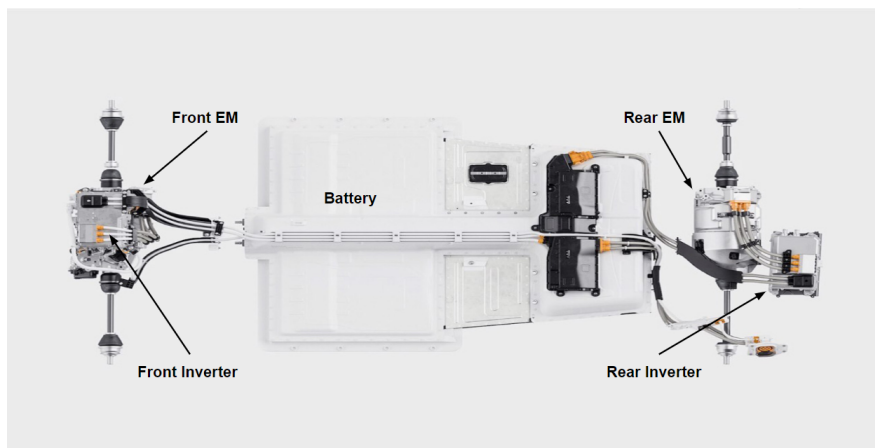


Figure 2.2.2: The hydraulic brake by wire brake system in Polestar 2.

A regenerative braking technology can be seen in various electric vehicles today, where the primary goals are to have a safe brake system and to recuperate as much energy as possible. Improvements towards a cleaner energy consumption is needed in order to improve environmental aspects. These improvements could be to increase the efficiency of certain systems. There are studies which show that approximately one third to one half of the power plant energy is used when braking. It is where the regenerative braking system comes into play, since it offers the possibility to convert the kinetic energy, which would otherwise be converted into heat, into electric energy and thereby improve fuel economy.[5]

As mentioned above, most electric vehicles use regenerative braking, however, in order to assure that the deceleration process meets the requirements, frictional brakes are applied. This type of system is often referred to as a "blended" brake system.

A blended brake system is used (frictional brake system and regenerative brake system) and it is therefore important that both systems are well integrated with one another. Hence, the structure of both systems are of importance for when a control strategy is considered. The control strategy has to be effective and based on an appropriate brake system, to achieve good results. The brake torque from the regenerative brake system and the frictional brake system have to be synchronized to fulfill the braking request from the driver and to optimize the regeneration. The brake torque provided from the electric motor needs to be regulated in order to fit the variations in torque from the frictional brake system [5].

2.3 The electric motor and its properties

The electric powertrain of the Polestar 2 consists of two 150 kW/330 Nm electric motors, where each axle consists of one electric motor (EM). The EM is a permanent magnet brushless DC motor, which is commonly used in electric vehicles due to its high efficiency, low wear and high specific power output [16].

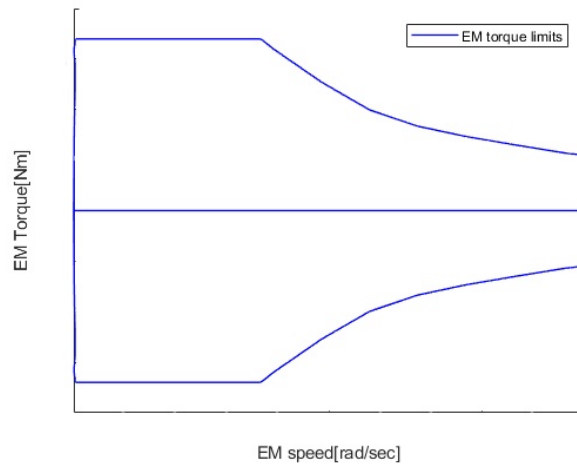


Figure 2.3.1: Plot of the torque output from the electric motor, which has a maximum value of 330 Nm.

The EM will have a constant peak output value from zero to a specific EM speed. Then at EM speeds which reach values outside of this interval the torque output will gradually start to decrease. This can be seen in Figure 2.3.1, where the torque starts to dip. Mathematically, the torque limit can be expressed as

$$M_{EM_j \min}(\omega_{EM_j}(\omega_i)) \leq M_{EM_j} \leq M_{EM_j \max}(\omega_{EM_j}(\omega_i)) \quad (2.13)$$

where $M_{EM_j \min}$ and $M_{EM_j \max}$ are nonlinear functions, typically given as lookup tables. The EM speed is directly related to the speed of the wheels through the differential gears.

The EM functions as an actuator during drive mode, while it is used as a generator during regenerative braking mode. During drive mode, the torque can be estimated

with the help of the first order equation seen below [17]

$$\dot{M}_{EM_j} = \frac{M_{EMreq_j} - M_{EM_j}}{\tau_{EM}} \quad (2.14)$$

where M_{EMreq_j} is the requested electric motor torque and τ_{EM} is the EM time constant.

2.3.1 Electric power storage system

The battery is the electrical motors power source. A battery model is provided by Volvo, and is used for this masters' thesis. The battery State of Charge (SOC) will be set to a constant value, as mentioned in the delimitation section. Hence, no limiting factors imposed by the battery will be considered.

2.4 Anti-lock braking system

The purpose of the ABS is to achieve the shortest longitudinal stopping distance while maintaining vehicle stability during deceleration. This is achieved by implementing a feedback control for the slip, which can control the slip at the point where maximum brake torque is employed on the wheel. The ABS model used in this thesis is referred to as ABS-soft. The ABS-soft model is based on single wheel dynamics, where it provides each wheel with a brake torque request. This section will provide with information about the ABS-soft model and its functionalities.

2.4.1 ABS-soft control strategy

The control strategy is based on a trigger criterion which combines wheel deceleration and slip control. This is done with the help of weighting factors, the expression seen in equation 2.14 is a representation of the control strategy [18].

$$S_i = K_{\dot{\omega}}\dot{\omega}_i + K_{\lambda}\lambda_i \quad (2.15)$$

where $K_{\dot{\omega}}$ and K_{λ} are weighting factors.

The desired value of S_i is between 0.15 – 0.2, this is the region where the optimal adhesion utilization is achieved. The model is built such that the brake pressure is reduced, released or maintained, in order to maintain S_i in the desired region. The ABS-soft model contains a subsystem where the driver brake input is converted in order to perform slip control. The driver is giving brake torque input to the model when full braking is applied. A filter is constructed, where a torque update is performed. The brake torque driver input is sent to the filter as pulsations between zero and max. The pulsations are decided by either reducing or releasing the pressure. The second input to the filter is a constant value, which is sent when the pressure should be maintained. The ABS-soft output for each wheel is described in the following equation

$$M_{ABS_i} = f_{ABS}(M_{dem_i}, S_i(\dot{\omega}_i, \lambda_i(\omega_i))) \quad (2.16)$$

where M_{dem_i} is the brake torque demanded at wheel i , M_{ABS_i} is brake torque requested by the ABS-soft model.

The goal of this project is to split the torque request by the ABS controller into friction and regenerative braking, i.e.

$$M_{ABS_i} = M_{fric_i} + \frac{M_{EM_j}}{2} \quad (2.17)$$

where M_{fric_i} is the brake torque request sent to the frictional brake system. Since the frictional brake system has no dynamics modelled it yields that the request is equal to the actual brake torque provided by the frictional brake system. The right-hand side terms in equation (2.17) are identical to the right-hand side terms in equation (2.10), giving that

$$M_{ABS_i} = M_{wheel_i}. \quad (2.18)$$

2.4.2 Torque output of the ABS-soft model

Figure 2.4.1 and 2.4.2 are a representation of the M_{ABS_i} determined by the ABS-soft model. These torques will be fundamental to construct a proper torque distribution controller. From Figure 2.4.1 it can be seen that the ABS intervention is initiated at 12s and terminated when the vehicle has stopped at approximately 15s. The brake torque then transitions from the ABS-soft request of 3000 Nm to full braking with a brake torque of 6000 Nm, which explains the peak at 16s.

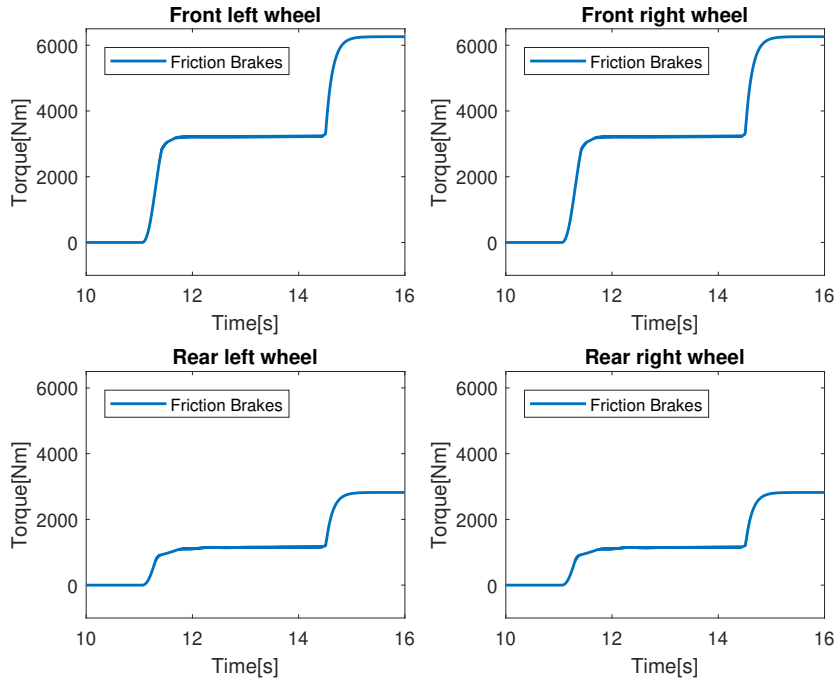


Figure 2.4.1: This figure is visualization of how M_{ABS_i} is divided between each frictional brake for each wheel, during a brake application which includes ABS intervention. The curve is plotted after 10s since the ABS intervention is initiated at 12s and terminated when the vehicle has stopped at approximately 15s.

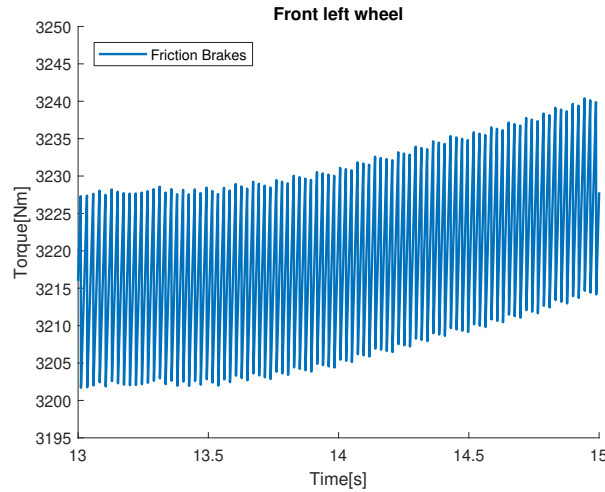


Figure 2.4.2: A representation of the pulsations (similar pulsations in all wheels) in the demanded torque for the front left wheel, caused by ABS-soft. The frequency is determined by how often the pressure has to be maintained, reduced or released in order to perform slip/wheel-control. The pulsations are presented at a randomly selected time interval from the time period where these pulsations occur.

2.5 Longitudinal dynamics during zero steering and constant heading

In this work a study of a simplified scenario where the vehicle yaw rate, yaw angle and steering angle are zero was performed, i.e. $\dot{\psi} = 0$, $\psi = 0$, $\delta = 0$. Then, it holds

$$F_{x_i} = F_{l_i} = \mu_i(\lambda_i(\omega_i, v))F_{N_i} \quad (2.19)$$

$$v_{l_i} = v_{x_i} = \dot{x} = v \quad (2.20)$$

where v is the vehicle speed and the function λ for computing longitudinal slip has been defined in (2.11). The vehicle equations of motion then simplify to

$$\dot{v} = \frac{1}{m} \sum \mu_i(\lambda_i(\omega_i, v))F_{N_i} \quad (2.21)$$

$$\dot{\omega}_i = \frac{1}{J_i} (-\mu_i(\lambda_i(\omega_i, v))F_{N_i})R + M_{ABS_i} - b_d\omega_i \quad (2.22)$$

$$\dot{M}_{EM_j} = \frac{M_{EM_req_j} - M_{EM_j}}{\tau_{EM}}. \quad (2.23)$$

Here, v , ω_i and M_{EM_j} are states in the system, M_{EMreq_j} is the controllable input and M_{ABS_i} and F_{N_i} are uncontrollable inputs, i.e. they are decided by other controllers or system dynamics. Recall that the EM torque is bounded

$$M_{EM_j \min}(\omega_{EM_j}(\omega_i)) \leq M_{EM_j} \leq M_{EM_j \max}(\omega_{EM_j}(\omega_i)) \quad (2.24)$$

as well as the requested EM torque

$$\frac{M_{EM_j}}{2} \geq M_{ABS_i} \quad (2.25)$$

which derives from the fact that the friction torque is nonpositive.

Notice that, if M_{EM_j} is decided, then the wheel friction torque is readily available from (2.17).

2.6 Brake blending during ABS

Brake blending in today's vehicle is not active during an ABS situation, this is due to not having any unforeseen issues. Figure 2.6.1 shows how brake-blending works, however during ABS M_{EMreq_j} is zero. M_{dem} is divided between front and rear axle, 70%/30%. The ABS block calculates the torque that is actually needed if the car starts to slip in order to prevent the wheels from locking. Torque split divides the torque from the ABS between the EM and the friction brakes. At every wheel there is a speed sensor that calculates the wheel speed and sends it back as a feedback to the controller. The car velocity is estimated as well in order to compare it to the wheel speed and calculate the slip.

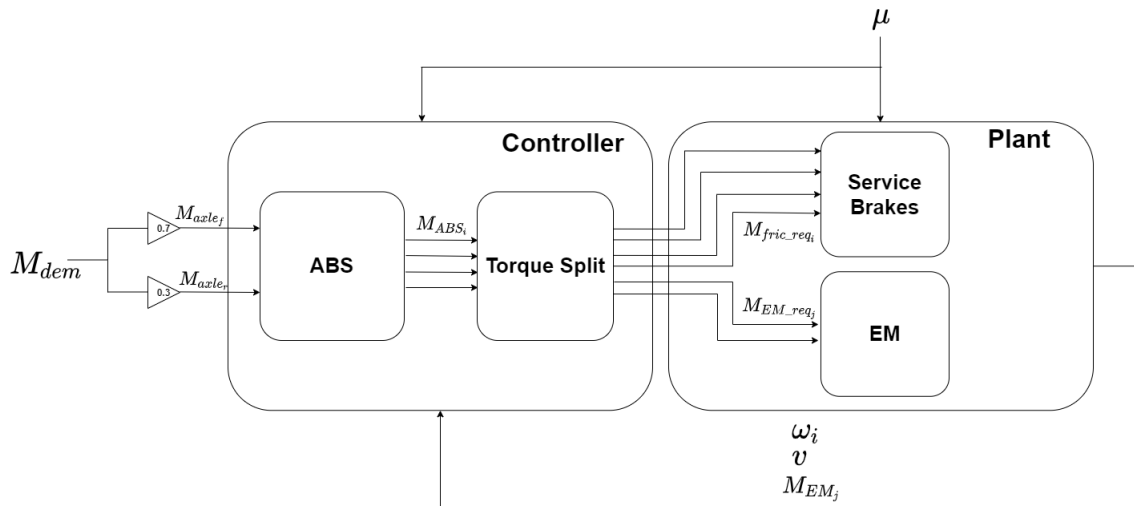


Figure 2.6.1: Control block diagram of the brake-blending system

2. Vehicle powertrain and braking system

3

Methods

3.1 Preliminary analysis regarding the implementation of a torque distribution controller

As the Simulink model provided by Volvo is very extensive, this model was studied to understand how to implement the control logic. It contains the powertrain of Polestar 2. The friction brakes is a part of CarMaker, meaning that a connection between the model and CarMaker was needed to perform analysis involving brake blending. The brake blending controller was implemented inside of the CarMaker blocks. Hence, the earlier mentioned connection is between the plant in the Simulink model and the control logic. The torque signals from the EM are used as an input and the brake request from the control logic to the EM is the output, meaning that it is a closed loop.

Proper subsystem connections within the model are of great importance, while for an extensive model the complexity of making valid connections increases. This implied that a lot of signal routing was required. An example of why proper connections are important, is when the EM brake torque request has to be sent to the transmission in order to receive a correct amount of brake torque. If the signal is incorrectly routed past the transmission, a too small amount of brake torque will be provided by the EM since a gear is used in the transmission to produce more brake torque. Connections like the one mentioned in the example have all been taken into consideration and thereby provided for the prerequisites required for constructing a torque distribution controller.

3.2 General torque distribution approach

As mentioned previously (see Section 2.2.1), an electric vehicle that uses brake blending, is often equipped with a brake by wire system in order to achieve ideal brake torque distribution. Brake torque distribution affects the efficiency and stability of the regenerative braking system, meaning that it is of utmost importance. The allocation between rear and front brake torque distribution will also have an impact on the stopping distance, vehicle directional control, the durability and thermal load on the brakes. The stopping distance is improved by optimizing the use of adhe-

sion, while over-braking an axle can cause steering and stability problems. Lastly the regenerative braking predominantly affects the strongest braked axle in terms of brake wear and thermal load [11].

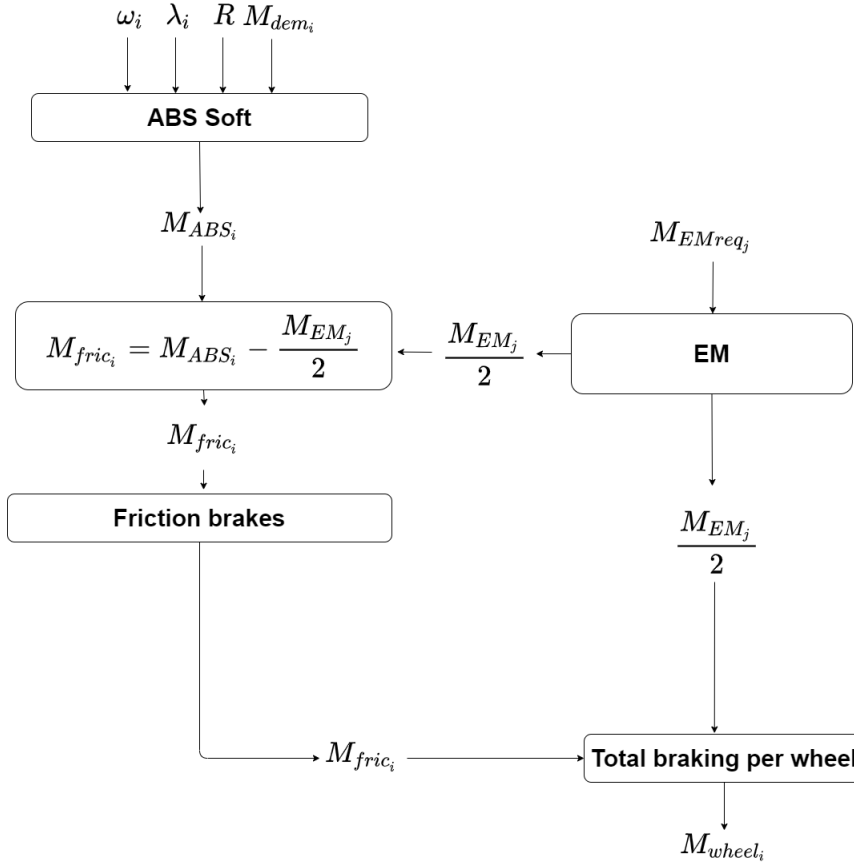


Figure 3.2.1: The signal-path is from top to bottom. M_{ABS_i} , is dependent on variables such as ω_i , λ_i , R and M_{dem_i} . The ABS-soft model calculates the requested torque M_{ABS_i} and the EM provides the brake torque $\frac{M_{EM_j}}{2}$ based on the brake torque request M_{EMreq_j} . M_{EM_j} is then subtracted from M_{ABS_i} and the remaining part of M_{ABS_i} is sent to the frictional brake system as M_{fric_i} . The frictional brake system then sends M_{fric_i} and $\frac{M_{EM_j}}{2}$ is added to provide with M_{wheel_i} .

The flowchart seen in Figure 3.2.1, visualizes how brake torque requests are handled by ABS-soft and distributed between the EM and friction brakes, where all of the brake torques in Chapter 3 are considered as positive. It can be seen how the ABS-soft requested torque for each wheel, M_{ABS_i} , is dependent on variables such as ω_i , λ_i , R and M_{dem_i} . The ABS-soft model calculates the requested torque M_{ABS_i} and the EM brake torque $\frac{M_{EM_j}}{2}$ is then subtracted from M_{ABS_i} . The remainder of M_{ABS_i} is then sent to the frictional brake system as M_{fric_i} , this is derived with the help of equation (3.1). The frictional brake system then provides M_{fric_i} and together with $\frac{M_{EM_j}}{2}$ adds up to M_{wheel_i} . The brake request sent to the EM, M_{EMreq_j} , will later on

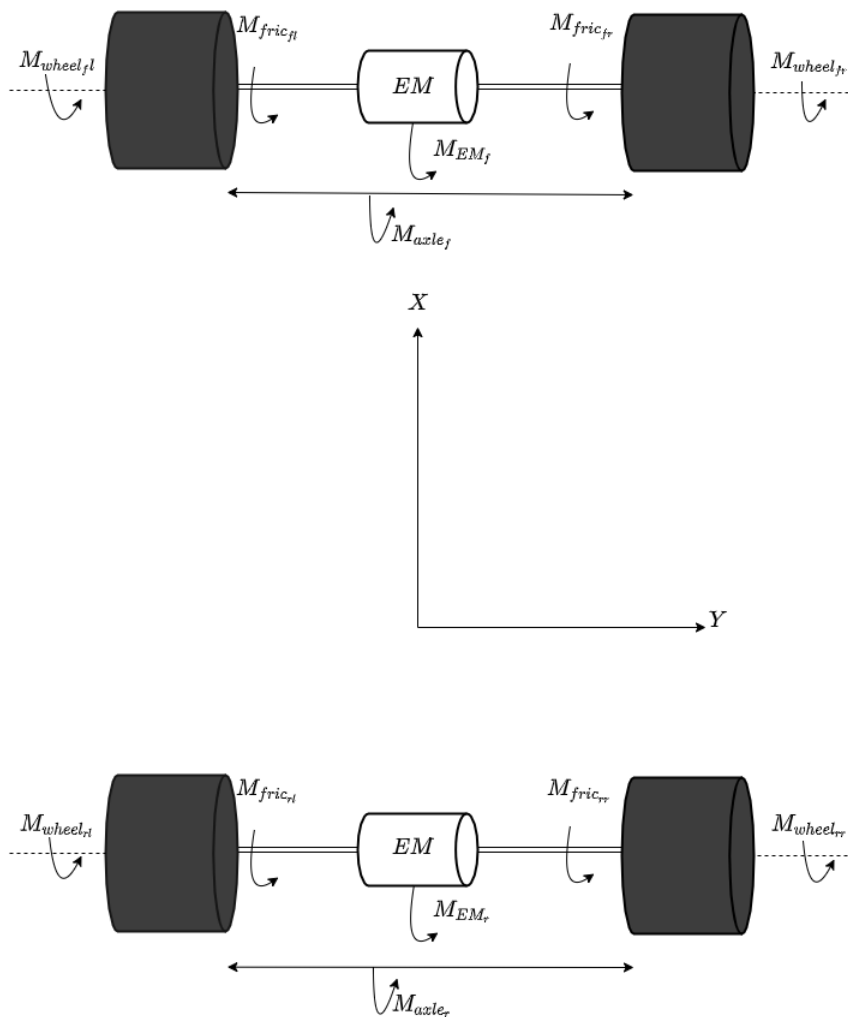


Figure 3.2.2: Schematic view of complete brake system, including a visual representation of the brake torque distribution.

be sent in two different ways, seen in sections 3.3 – 3.4, where two different control methods are presented.

A regenerative brake system should be able to reach the goal of the required brake torque, while recuperating as much energy as possible. The system needs to output the right amount of braking torque in order to meet the requirements during deceleration. As mentioned before, brake torque for each wheel needs to be distributed properly in order to maintain vehicle stability. When these two requirements are fulfilled, then energy regeneration can be optimized to recuperate as much energy as possible. [11].

Figure 3.2.2 is a visualization of the entire brake system and brake torque distribution.

The total requested brake torque is provided by the electric motor and the frictional brakes, the expression seen in equation (3.1) shows how the torque from the electric

motor and the friction brakes is combined to the requested brake torque from the ABS-soft, which will be the actual brake torque on the wheel

$$M_{wheel_i} = M_{ABS_i} = M_{fric_i} + \frac{M_{EM_j}}{2} \quad (3.1)$$

There are three approaches explored in this project. The control, Approach I, is when all of the torque is provided by the friction brakes. This means that no brake torque is provided by the electric motor, and no brake blending is used. The amount of brake torque on each axle is expressed in equations (3.2), (3.3) and the total brake torque is then the sum of the brake torque from each axle, seen in equation (3.4).

$$M_{axle_f} = M_{fric_{fl}} + M_{fric_{fr}} + M_{EM_f} \quad (3.2)$$

$$M_{axle_r} = M_{fric_{rl}} + M_{fric_{rr}} + M_{EM_r} \quad (3.3)$$

$$M_{ABS_{tot}} = M_{axle_f} + M_{axle_r} \quad (3.4)$$

The total brake torque demanded by the ABS model, $M_{ABS_{tot}}$, is 70%/30% between front and rear axle. The front left and right wheel friction brakes, will receive the same brake torque. The rear friction brakes will follow the same principle. The expressions seen in (3.2)-(3.4), can then be derived to equations (3.5) and (3.6)

$$0.7M_{ABS_{tot}} = M_{axle_f} \implies M_{fric_{fr}} = M_{fric_{fl}} = \frac{0.7M_{ABS_{tot}} - M_{EM_f}}{2} \quad (3.5)$$

$$0.3M_{ABS_{tot}} = M_{axle_r} \implies M_{fric_{rr}} = M_{fric_{rl}} = \frac{0.3M_{ABS_{tot}} - M_{EM_r}}{2} \quad (3.6)$$

3.3 Approach II, Brake Blending with maximal usage of the electric motor

The flowchart seen in Figure 3.3.1, visualizes the torque distribution referred to as Approach II. This distribution logic is built in order to achieve brake blending, where both the EM and friction brakes are used in parallel during the entire brake application. The brake request provided by the ABS-Soft model, M_{ABS_i} , is sent directly to the EM. The goal is to utilize as much regenerative braking as possible. The brake torque provided by the EM, M_{EM_j} is subtracted from the brake torque request from the ABS-soft model, M_{ABS_i} . After M_{EM_j} is removed from M_{ABS_i} , the rest, M_{fric_i} is sent directly to the friction brakes. Then the frictional brake system gives M_{fric_i} and together with $\frac{M_{EM_j}}{2}$ adds up to M_{wheel_i} .

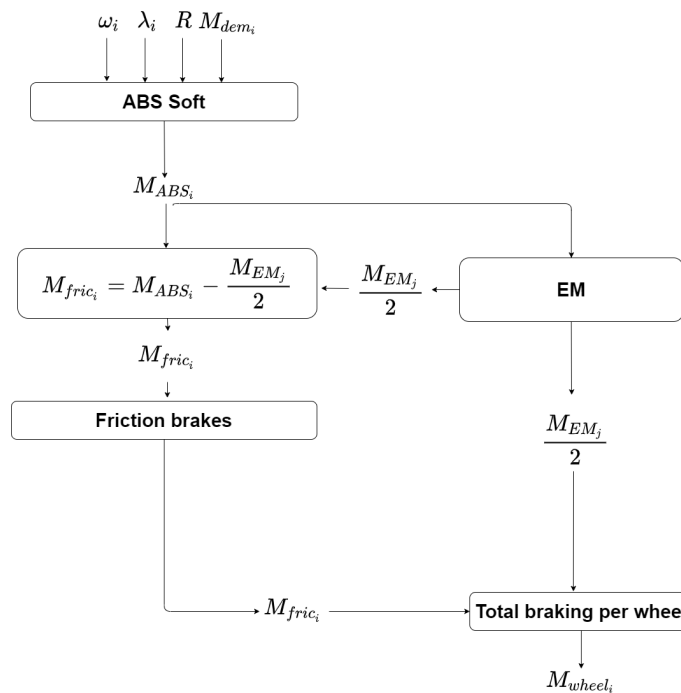


Figure 3.3.1: Flowchart representation of Approach II. The signal-path is from top to bottom. The torque request from ABS-soft, M_{ABS_i} , is dependent on variables such as ω_i , λ_i , R and M_{dem_i} . The ABS-soft model calculates the requested torque M_{ABS_i} and the EM provides the brake torque $\frac{M_{EM_j}}{2}$ based on the brake torque request $M_{EM_{req_j}}$. M_{EM_j} is then subtracted from M_{ABS_i} and the remaining part of M_{ABS_i} is sent to the frictional brake system as M_{fric_i} . The frictional brake system then sends M_{fric_i} and $\frac{M_{EM_j}}{2}$ is added to provide with M_{wheel_i} .

3.3.1 Switch implementations necessary for a beneficial torque distribution

Since M_{EM_j} is sent directly from the EM to the logic, certain switches needed to be made. These switches were implemented to constrain the model to be used only during braking. The restrictions are required because the EM is used during acceleration. Since M_{ABS_i} is zero during acceleration, then M_{EM_j} is subtracted from M_{ABS_i} , resulting in a negative brake request to be sent to friction brakes. This is the reason why the logic only can be activated during braking. Three different switches have been implemented and are visible in Figures 3.3.2, 3.3.3 and 3.3.4. Switch I and II, are applied in Approach II, while all the switches are applied in Approach III (presented in section 3.4).

The switch seen in Figure 3.3.2 was made to prevent the distribution logic from applying any torque from the EM used to accelerate. This basic switch, passes through the maximal value of M_{EM_j} and 0 as an output, hence M_{EM_j} can only be an output if it is positive valued (braking).

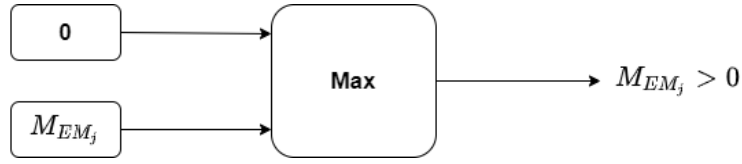


Figure 3.3.2: This figure visualizes the switch-logic, which starts from left by sending a constant value of 0 and the torque produced by the EM, M_{EM_j} , to the block to its right, which sends the maximal value of the two inputs.

The second switch seen in Figure 3.3.3, prevents the distribution logic from sending a negative brake torque request to the friction brakes. Since the electric motor is used for acceleration and deceleration, there is a time-consuming transition from one to the other. The EM has to transition from a high torque application used for acceleration, giving a negative M_{EM_j} , to a zero-crossing point (where the sign of a function is flipped), to a state were it produces brake torque instead. This is the reason that the switch was implemented, since the effect of zero crossing has to be considered.

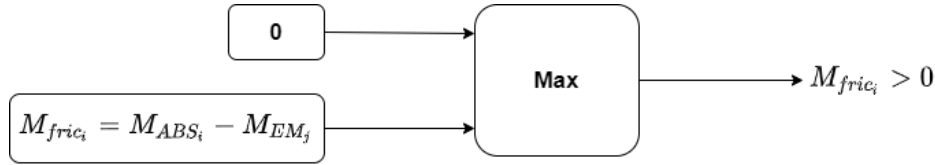


Figure 3.3.3: A visualization of the switch-logic constructed with the cause of preventing negative M_{fric_i} to be sent to the friction brakes. The logic starts with the left side, where a constant value of zero and the difference between M_{ABS_i} and M_{EM_j} , are used as inputs to the max block. The max block then gives a positive value M_{fric_i} as an output.

The third switch was constructed as a system activator. No brake request, M_{EMreq_j} , is sent to the EM unless brake pressure is applied. This switch triggers the torque distribution by sending a request to the EM as soon as the driver applies brake pressure.

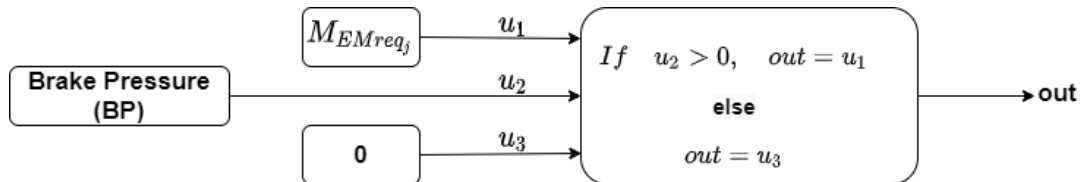


Figure 3.3.4: This figure is a visual representation of the "system activator", where the three inputs to the left are, M_{EMreq_j} (u_1), Brake Pressure (BP), (u_2) and a constant value of zero (u_3). These are the inputs to the switch following to the right, where it gives an output of M_{EMreq_j} if BP is larger than 0, else a constant value of 0 is the output.

3.4 Approach III, Brake Blending with a regulated usage of the electric motor

In Approach II the amount of brake torque sent by the EM was directly influenced by the brake torque request given by ABS-soft (M_{ABS_i}). Meaning that the brake torque request sent to the EM was not regulated. Approach III was developed to have the ability to regulate the brake torque request sent to the EM. Approach III has similarities to Approach II in terms of removing M_{EM_j} from M_{ABS_i} and sending the rest to the friction brakes. However, Approach III has several different key features compared to Approach II such as, a lookup table, constant brake torque corresponding to each road surface, and EM limitations containing a converter since the requested brake torque M_{EMreq_j} passes through a transmission. The EM brake torque request, M_{EMreq_j} , is determined by using a lookup table and is a constant value depending on the road surface. The control logic is presented by the flowchart seen in Figure 3.4.1 and is a representation of a single wheel.

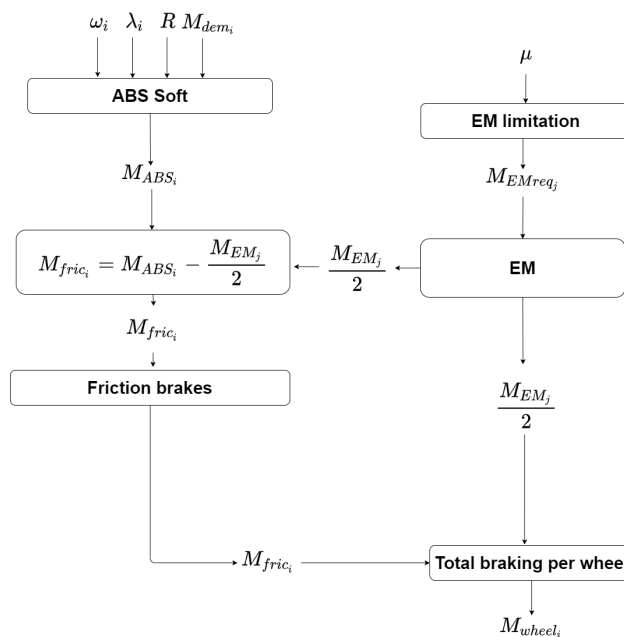


Figure 3.4.1: The figure is a flowchart visualization of the torque distribution strategy developed for Approach III. The flow starts from the top, divided in two pathways, one where the M_{ABS_i} is sent directly to the distribution block and the other where the constant M_{EMreq_j} is calculated first and then sent to the EM. The EM then sends a constant brake torque $\frac{M_{EM_j}}{2}$, which is removed from M_{ABS_i} in order to send the rest, M_{fric_i} , to the friction brakes. The frictional brake system then returns M_{fric_i} and together with $\frac{M_{EM_j}}{2}$ provides M_{wheel_i}

3.4.1 Calculation of constant electric motor torque

In Approach III, the EM is used to send a constant brake torque during the application of the brakes. M_{EM_j} is removed from the M_{ABS_i} in order to send the rest, M_{fric_i} , to the friction brakes. The constant brake torque M_{EM_j} must be below the minimal values of the oscillations in the M_{ABS_i} , since the oscillations should be handled by the friction brakes. If an acceptable M_{EM_j} is achieved, it implies that a valid removal from the M_{ABS_i} was performed. In order to find the value for M_{EMreq_j} , an extreme-value function was developed. The extreme-value function determines $M_{EMreq_j} * gear$, where $gear$ is the scaling factor found in the transmission in the EM. The lookup table was used to store these constant EM brake torque requests scaled by $gear$ (referred to as M_{lookup_j}) for different road surfaces, which should reduce computational cost by being able to provide the EM with a brake torque request as soon the brake application is initiated.

3.4.1.1 Achieving a desired brake torque request using an extreme-value function

Different road surfaces will result in different M_{ABS_i} , meaning that different M_{EM_j} are required. This is solved by developing an extreme-value function with the help of a MATLAB script. The function works as follows: it finds the max value under the oscillations (caused by the ABS front/rear brake request) plus a fixed margin and then sets it as an element of an array. Each element in this array is a different M_{lookup_j} corresponding to a road friction coefficient. The array is then used as an output in a lookup table. This is implemented to prevent the logic from sending a too large brake torque request to the EM and also to keep the oscillations from crossing the constant request. This can be seen in Figure 3.4.2.

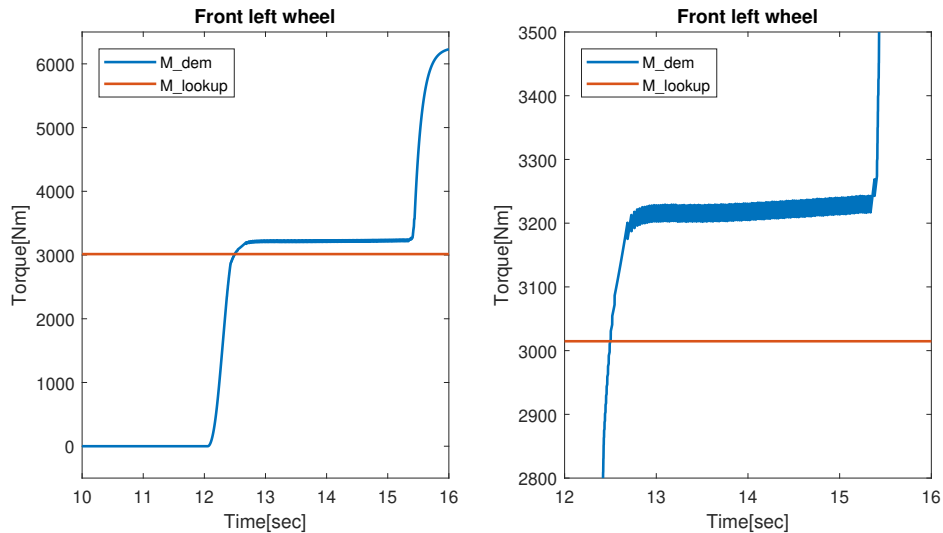


Figure 3.4.2: The figure is a representation of how the extreme-value function is choosing M_{lookup_j} (red line) right before the oscillations seen in the demanded torque (blue curve).

3.4.1.2 Test on different road friction coefficients

Several values of friction coefficients were used during simulation, all within a range from 0.5 to 1, increased step-wise by 0.1. This gives a more robust model in terms of braking on different road surfaces.

3.4.1.3 Regulating brake torque request using a lookup table

Each friction coefficient will be passed as an input variable to a lookup table. The road friction coefficient is the only input, making the table 1-Dimensional. A value corresponding to the input is then the output from the table, yielding the desired M_{lookup_j} . If the step-size for choosing a new road friction coefficient is decreased from 0.1 to a smaller value, the lookup table will, by using interpolation output a value based on the two neighbouring values.

3.4.1.4 Consideration of electric motor limitations

The EM limitations, in terms of brake torque output was considered in the torque distribution controller, since a constant brake torque request implies that there exists a possibility of requesting an unreachable amount of brake torque during certain wheel-speeds. The flowchart seen in Figure 3.4.3 represents the entire subsystem step by step, where EM limitations are considered. A switch was implemented, where either a constant request set by the lookup table is chosen, or if the constraint set by the EM should be considered by sending maximal power output divided by wheel-speed instead.

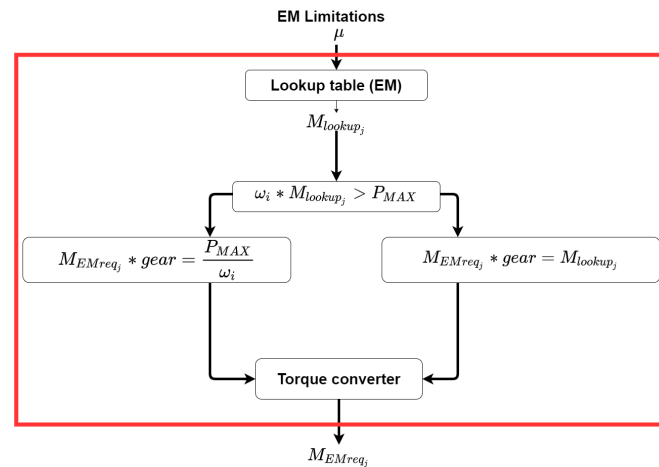


Figure 3.4.3: A flowchart representation of the EM limitations is presented inside the red square. The flow goes from top to bottom, starting with the road friction coefficient as an input to a lookup table, which then has the corresponding constant brake torque, referred to as M_{lookup_j} , as an output. M_{lookup_j} is then checked in the following block, if it can be realized or if it is limited by the EM. Depending on if it passes the condition or not, it can take two different pathways. Both of the paths goes through the Torque converter where $gear$ is removed and leaves M_{EMreq_j} , which is being sent directly to the EM.

3.4.1.5 Torque conversion using a gear ratio

The M_{lookup_j} generated from the subsystem where the EM limitations are considered, represents the amount of brake torque the EM can provide. This is the brake torque the EM can provide after the M_{EMreq_j} has passed through the transmission, where it is multiplied by a gear-ratio (*gear*). This is the reason why an inverse transmission was needed in order to convert the brake torque request to receive a correct brake torque.

3.5 Simulation tools used for model-construction and result provision

All models within this work were built using Simulink, while all parameters were defined and some functions were created in Matlab. CarMaker was used in order to provide driver inputs, i.e. acceleration and deceleration values. CarMaker was also used to create a testing environment, meaning that it was possible to easily alter road-conditions. All simulations were performed using CarMaker and the results from these simulations were visualised using CarMaker Movie. CarMaker Movie gives the user the possibility to visually experience the braking procedure. The visual function was used to study the behaviour of the car in terms of lateral displacements, which determines the vehicle's stability during braking, as the goal was to keep the vehicle moving in a straight line.

4

Results & Discussion

All of the presented results are simulated with a road friction coefficient equal to 1, except the ones presented in the Design of experiments (DoE). In order to compare brake blending and pure friction brakes during a ABS situation, different tests were made using CarMaker. Two types of tests were performed, one where the car drives with a speed of 130 km h^{-1} , releases the accelerator pedal and waits 1 second before applying brake pressure, and the other where the driver accelerates for 11 seconds, then immediately applies brake pressure.

- Test Case 1 where the driver waits one second before applying brake pressure, is used to better understand how the response time of the EM influences the braking distance, as this delay prevents zero-crossing of EM torque.
- Test Case 2 where brake pressure is applied instantly after using the EM for acceleration, this is a more realistic scenario, as it represents an emergency stop. This test case visualizes the zero-crossing of EM torque from Approach II and III.

Results of the torque distributions for the two control strategies are presented in Figures 4.1.1 - 4.1.2 and 4.2.1 - 4.2.2. Each of these figures consists of 4 sub-figures that represent each wheel. In each sub-figure different torque-graphs are shown both from brake blending (Approach II and III) and when only using friction brakes (Approach I). This is to compare an emergency brake situation with and without brake blending. All brake torque curves are plotted as positively valued, this is to get a clearer visualization of which brake system is used more during braking, since negative plot may be less clear. Graphs that show results from Approach I are referred to as "No brake blending" in the legend. For each wheel five curves are plotted:

- No Brake Blending - ABS Request: This curve represent the brake torque that the ABS requests when braking only with friction brakes ($M_{ABS_i} = M_{fric_i}$). This torque request is sent directly to the friction brakes.
- Brake Blending - ABS Request: This curve represent the brake torque that the ABS request when brake blending is implemented ($M_{ABS_i} = M_{fric_i} + \frac{M_{EM_j}}{2}$).
- Brake Blending - EM torque: This curve represents the EM brake torque

applied at each wheel ($\frac{M_{EMj}}{2}$).

- Brake Blending - Friction brakes: This curve represent the torque that is sent to the friction brakes. The torque is the difference between requested ABS torque and the EM torque ($M_{fric_i} = M_{ABS_i} - \frac{M_{EMj}}{2}$).
- Brake Blending - Total brake torque: This curve represent the EM torque and the friction Brakes torque add together ($M_{wheel_i} = M_{fric_i} + \frac{M_{EMj}}{2}$). It is used for comparison with the requested ABS torque.

4.1 Approach II, Brake Blending with maximal usage of the electric motor

4.1.1 Comparison of brake torque when using brake blending and when not using brake blending

This subsection presents and analyzes the results achieved regarding the torque distribution, whilst using the max amount of brake torque from the electric motor.

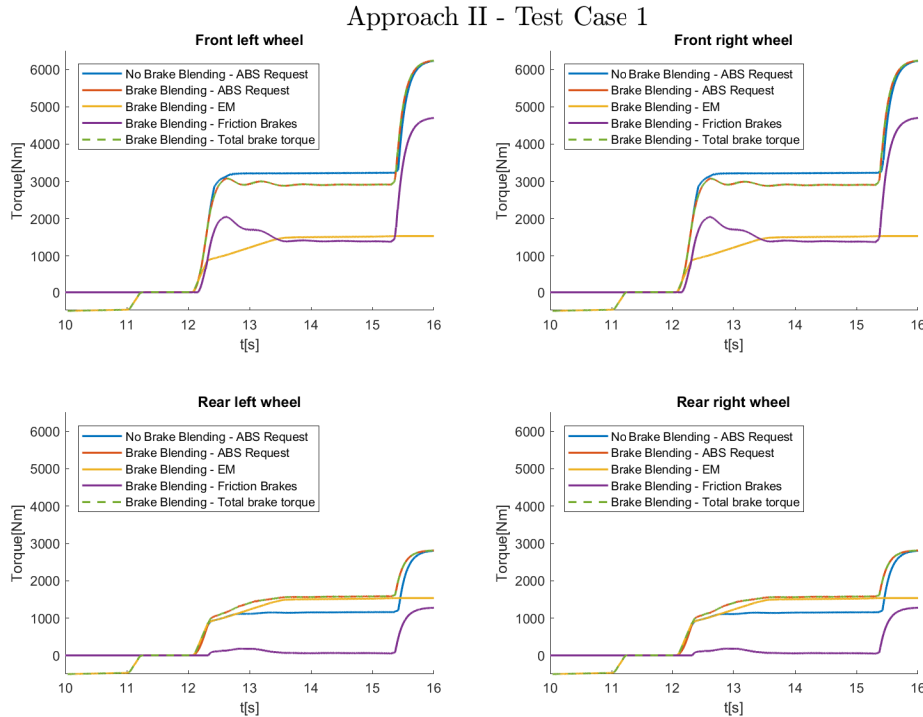


Figure 4.1.1: The figure is a representation of how Approach II performs during Test Case 1 compared to Approach I, where each subplot represents one of the wheels. The curve is plotted after 10s since the brake application starts at time $t \geq 12$ s and is terminated when the vehicle has stopped at approximately 15s. The one second pause interval starts at $t \approx 11$ s and ends at $t \approx 12$ s, the brake application therefore starts at time $t \geq 12$ s.

Since it can be seen from Figure 4.1.1 that the EM responds quicker than the friction brakes during blending, one may expect that Test Case 1 will be more effective in terms of braking distance compared to Test Case 2. This is since the EM has a faster response time than the friction brakes and does not need time to transition from acceleration to deceleration (zero crossing) for Test Case 1.

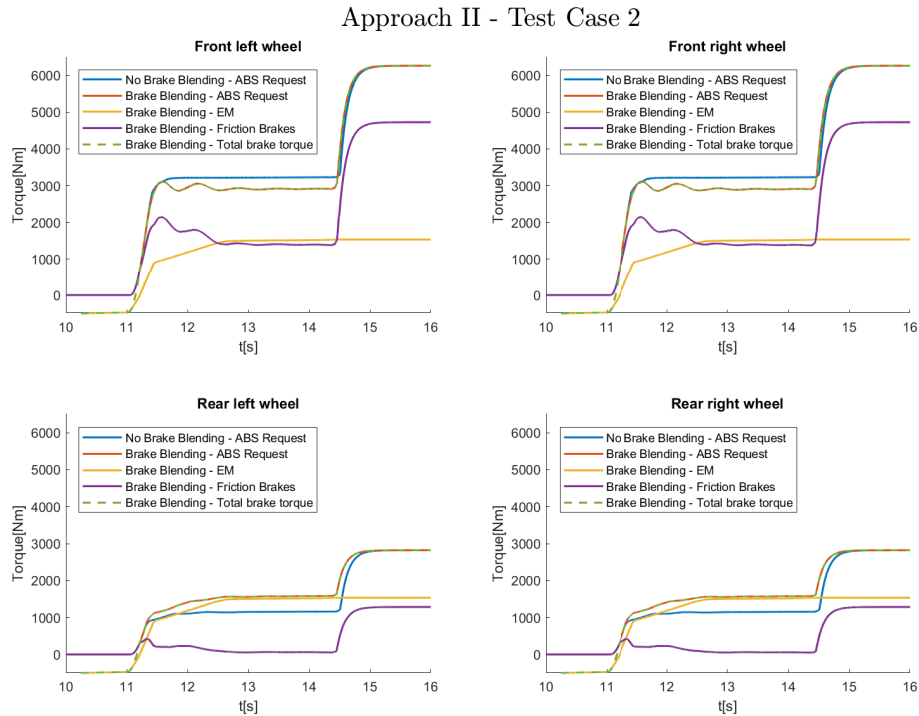


Figure 4.1.2: The figure is a representation of how Approach II performs during Test Case 2 compared to Approach I, where each subplot represents one of the wheels. The curve is plotted after 10 s as the brake application starts at time $t \geq 11$ s and is terminated when the vehicle has stopped at approximately 14.5 s.

Figure 4.1.2 visualizes the torque distribution for Test Case 2, where the driver brakes instantly after accelerating. It can be seen that the no brake blending ABS request differs from the brake blending torque request. When brake blending is used, oscillations are present in the ABS torque request for the front axle, these oscillations are higher compared to the ones in the rear axle. The reason this occurs is unclear, as this behaviour is not typically expected, and the request is provided by ABS-soft, which tries to control the slip and wheel-deceleration. By looking at the plot it can be seen that it takes time for the EM to transition from an accelerating to a decelerating state. Hence, the EM starts to brake later than the friction brakes. This means, that all the braking during this transition is handled by the friction brakes. This was expected behaviour because a switch was implemented in order to disregard any EM torque used during acceleration. It can also be seen that the friction brakes provide only a small portion of brake torque when compared to the EM, when brake blending is used. This is because the ABS request is sent directly

to the EM, which then sends the most brake torque possible.

The results seen from Approach II imply that the EM has a quicker response time than the friction brakes. This is seen in Figure 4.1.2 where a one second pause is applied, the EM responds faster than the friction brakes. This is because the EM had time to stop giving negative brake torque (acceleration) in the one second pause, and is thereby able to produce brake torque as soon the driver applies brake pressure. The EM is faster, which implies that the car starts to decelerate sooner when brake blending is used, as opposed to when only friction brakes are applied. It can be noted that the EM uses a constant brake torque for both scenarios, unless the EM limitations stops the EM from providing the requested amount of brake torque. In the resulting plots there are two different slopes visible during the time interval 11.5 s to 16 s. The reason the EM gives constant brake torque is due to the request that it receives. The ABS request is sent directly to the EM requesting a higher brake torque than what the EM is capable of. This makes the EM send its maximum amount of torque (around 1500 Nm). Hence, a constant maximal brake torque is provided by the EM, as long as the limitations do not constrain it.

4.1.2 Comparison of slip when using brake blending and when not using brake blending

The slip comparison between the two cases and when no brake blending is applied, is presented in Figure 4.1.3 and is visualizing only the front left wheel. The tests were executed on a straight road with a constant road friction coefficient meaning that the difference in slip behaviour between the four wheels is negligible.

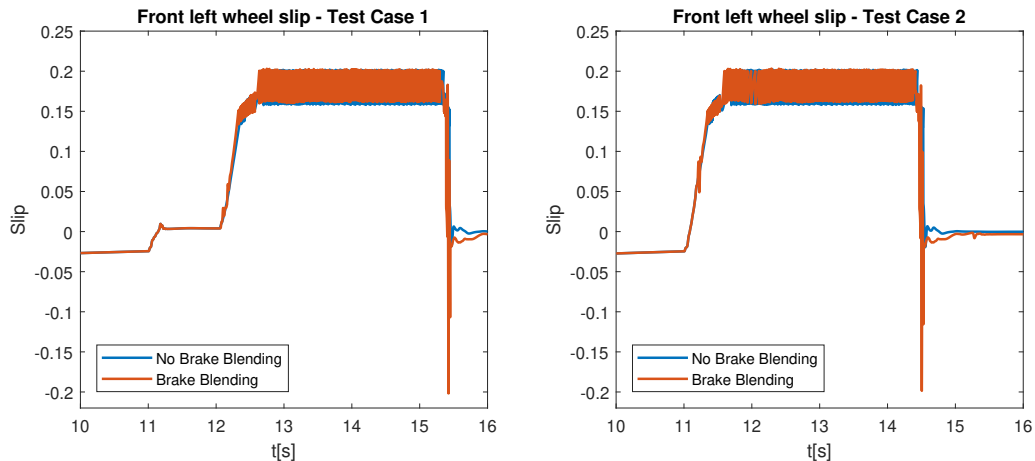


Figure 4.1.3: A visual representation of the slip comparison between Approach I and Approach II, for Test Case 1 (left plot) and Test Case 2 (right plot). Both plots are a representation of the front left wheel. The curves are plotted after 10s since the brake application starts at time $t \geq 12$ s for Test Case 1 and $t \geq 11$ s for Test Case 2. The one second pause interval for Test Case 1 starts at $t \approx 11$ s and ends at $t \approx 12$ s, when the pause interval is completed the brake applications is initiated. The brake application for Test Case 1 is terminated when the vehicle has stopped at approximately 15s and for Test Case 2 at approximately 14s.

From the the results seen in Figure 4.1.3 it can be seen that the slip during brake blending behaves as stable as no blending for both Test Case 1 and 2. The slip control is almost identical for both cases, except the part of the plot where either instant braking is applied or a pause of one second.

4.1.3 Deceleration when using brake blending and when not using brake blending

The deceleration comparison between the two cases and no blending, is presented in Figure 4.1.4. Very similar behaviour was seen between the brake blending and no brake blending for both test cases. The main difference is identified at the negative peak values from both plots, which implies that a greater brake torque is applied when brake blending is used. Thus, giving a shorter brake distance as can be seen in Figure 4.1.6, at around second 15, where the car has has stopped. The oscillations seen in the ABS demanded torque are also visible in the plot approximately between 12sec to 15sec on the Time-axis of the plot.

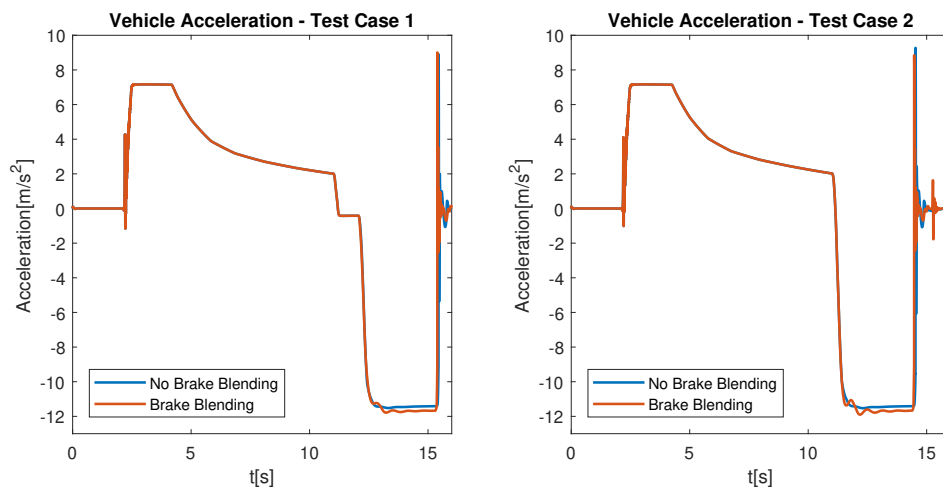


Figure 4.1.4: The figure is a representation of the resulting vehicle deceleration comparison, between Approach I and Approach II, during Test Case 1 (left plot) and Test Case 2 (right plot). The vehicle did not start to accelerate (positive valued curve) until $t \geq 2$ s for Test Case 1 and 2. The curves are plotted after 10 s since the brake applications starts at time $t \geq 12$ s for Test Case 1 and $t \geq 11$ s for Test Case 2. The one second pause interval for Test Case 1 starts at $t \approx 11$ s and ends at $t \approx 12$ s, when the pause interval is completed the brake application is initiated. The brake application for Test Case 1 is terminated when the vehicle has stopped at approximately 15 s and for Test Case 2 at approximately 14 s..

4.1.4 Comparison of velocity when using brake blending and when not using brake blending

In Figure 4.1.5 the velocity of the car is visualised. The difference in velocity between blending and no blending, for Test Case 1, differs approximately by $0.1 m/s$. The

same applies to Test Case 2. This a negligible difference in velocity and its affect on the brake distance is minimal.

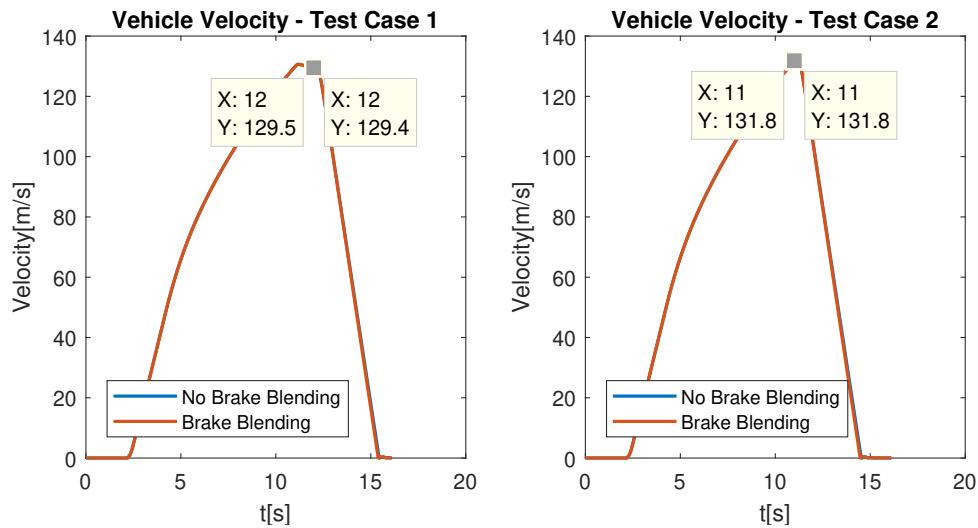


Figure 4.1.5: The figure is a representation of the resulting vehicle velocity when using Approach I and II, during Test Case 1 (left plot) and Test Case 2 (right plot). The vehicle does not start to accelerate until $t \geq 2$ s for Test Case 1 and 2. For Test Case 1 the one second pause interval starts at $t \approx 11$ s and ends at $t \approx 12$ s , when the pause interval is completed the brake applications starts at time $t \geq 12$ s . In Test Case 2 the brake application is initiated at $t \geq 11$ s . The brake application initiation is marked in both plots with a grey square, where it can be seen that velocity between Approach I and II differs for both cases.

4.1.5 Comparing brake distance when using brake blending and when not using brake blending

The results seen in Figure 4.1.6, implies that the torque distribution when the usage of the EM is maximized yields a shorter brake distance than without the brake blending. The decrease in brake distance differs from Test Case 1 to Case 2. The brake distance is decreased more in Test Case 1, where the one second pause is used, than during Test Case 2 where zero crossing occurs. As earlier discussed with the response time, it was expected that Test Case 1 with a one second pause will be more effective. This is because the brake torque provided can be applied earlier giving the vehicle a head-start compared to the scenario where zero crossing occurs. The scenario where zero crossing occurs doesn't yield as big of a improvement in terms of brake distance, but it still shortens the distance when compared to no blending. The reason being that the total brake torque demanded on the rear axle is higher when brake blending is used than for the scenario when no brake blending is used. As mentioned above, it can also be seen that the vehicle's deceleration is higher when the brake blending logic developed is used, which should imply a shorter distance and is a correlation to the higher usage of brake torque.

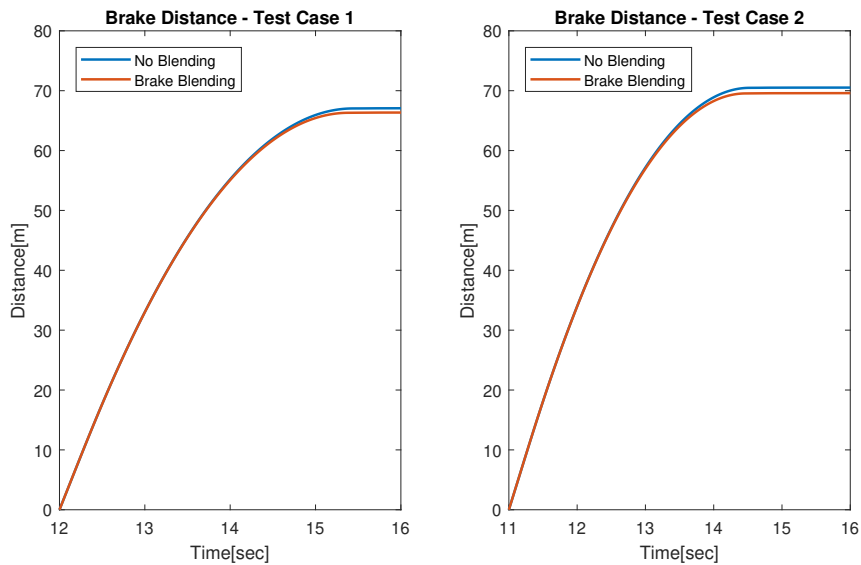


Figure 4.1.6: The figure is a representation of the resulting vehicle brake distance when using Approach I and II, during Test Case 1 (left plot) and Test Case 2 (right plot). The brake application starts at time $t \geq 12$ s for Test Case 1. In Test Case 2 the brake application is initiated at $t \geq 11$ s .

Figure 4.1.7 gives a clearer visualization of the brake distance decrease.

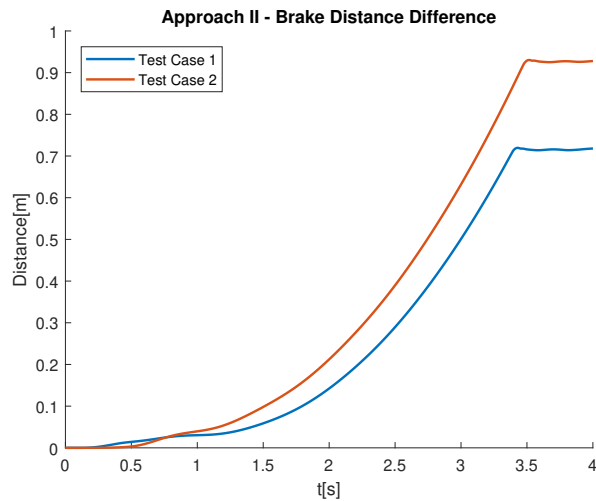


Figure 4.1.7: The figure is a representation of the brake distance difference between Approach I and Approach II for Test Case 1 and 2. The x-axis represents the time that the car is braking and the y-axis represents how big the difference is between the brake distance for Approach I and Approach II.

4.2 Approach III, Brake Blending with a regulated usage of the electric motor

4.2.1 Comparison of brake torque when using brake blending and when not using brake blending

This subsection presents the results achieved regarding the torque distribution using a regulated amount of brake torque from the electric motor.

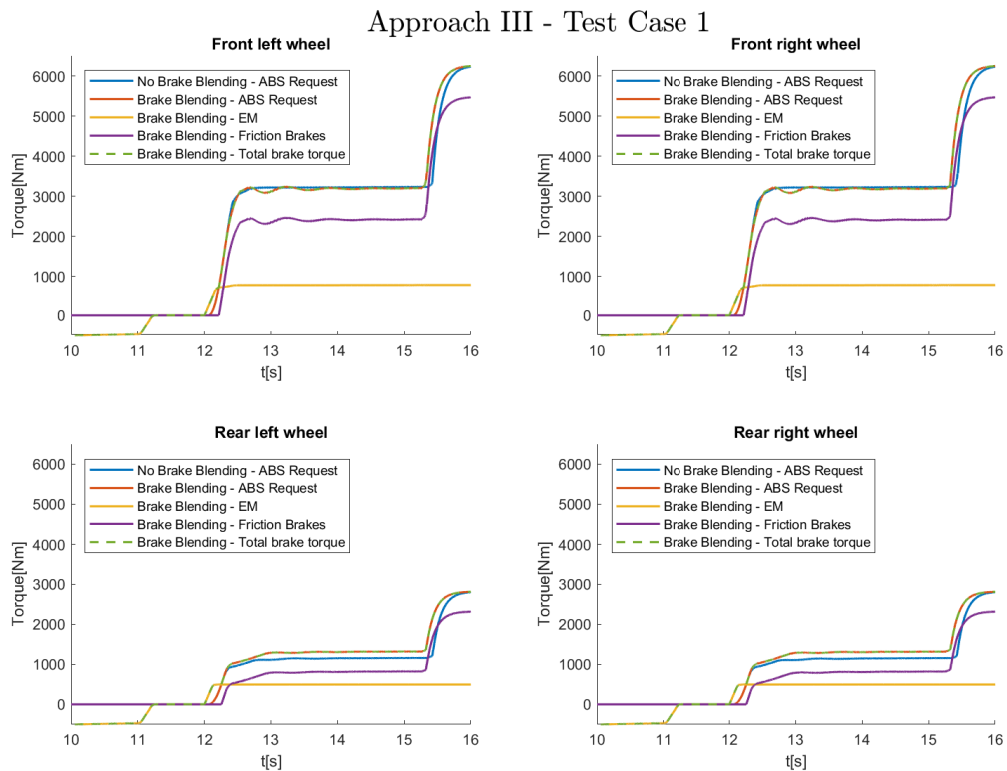


Figure 4.2.1: The figure is a representation of how Approach III performs during Test Case 1 compared to Approach I, where each subplot represents one of the wheels. The one second pause interval is starting at $t \approx 11$ s and ending at $t \approx 12$ s, when the pause interval is completed the brake applications starts at time $t \geq 12$ s

Figure 4.2.1 visualises that when using brake blending, the braking starts earlier since the EM begins to brake as soon as the driver presses the brake pedal. This is due to the switch, that allows a brake torque request being sent to the EM as soon as the driver decides to apply brake pressure. This makes the EM start braking before an actual brake torque request is sent by the ABS model. This switch can easily be changed such that the EM starts to brake as soon as the ABS request is larger than zero. This will decrease the significant head-start the EM has compared to the friction brakes. The current head-start has proven to decrease the brake distance effectively, but it can still affect the vehicle stability.

The total brake torque when brake blending is used has small pulsations as well bigger oscillations compared to the brake torque during braking with only friction brakes. It can be observed that for the front axle the torque request from the ABS during brake blending is approximately the same as the torque request from the ABS during braking with only friction brakes. This is however not the case for the rear axle. The torque request from the ABS during brake blending is higher than the torque request from the ABS during braking with only friction brakes.

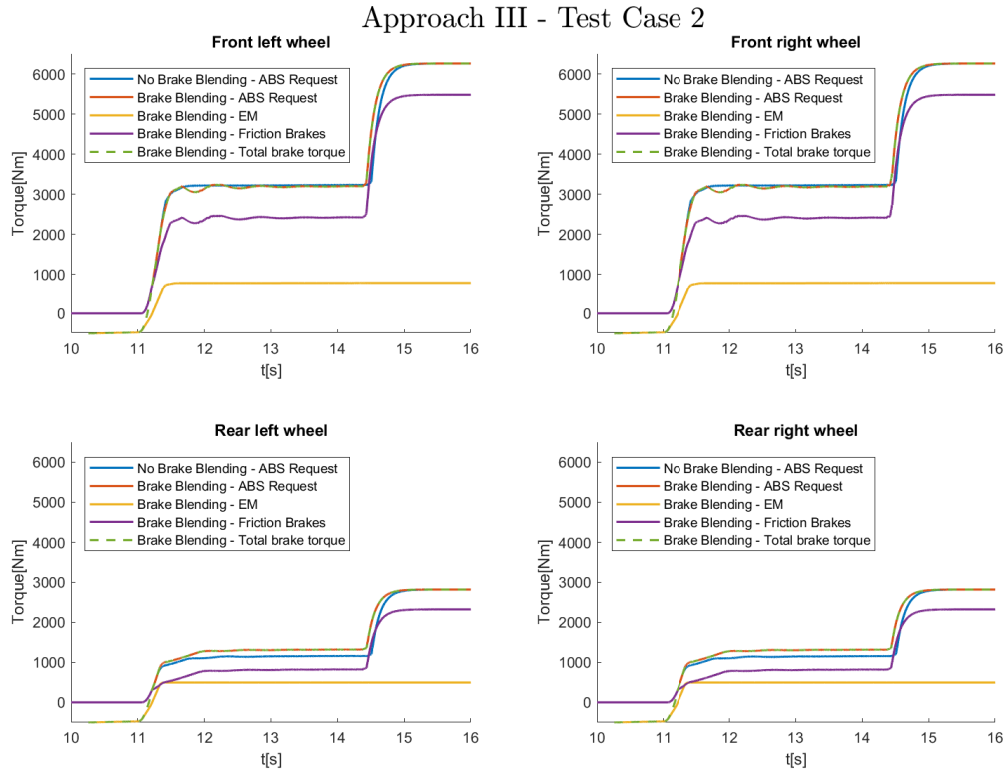


Figure 4.2.2: The figure is a representation of how Approach III performs during Test Case 2 compared to Approach I, where each subplot represents one of the wheels. The brake applications starts at time $t \approx 11$ s .

By looking at Figure 4.2.2 it can be seen that it takes time for the EM to transition from a accelerating to a decelerating state. Making the EM start to brake later than the friction brakes. Meaning, that all the braking during this transition is taken care of by the friction brakes which is a expected behaviour as explained in subsection 4.1.1.

During this work it was confirmed that the EM has a faster response time compared to the friction brakes. This is evident in both Approach II and III. The biggest difference between Approach II and III is the resulting brake torque distribution as shown in section 3.3 – 3.4 and thereby provides with different results. This further confirms the significance of a brake torque distribution.

The EM brake torque in Approach III behaved as expected, it was validated through simulations that the EM can produce a constant brake torque at different levels, where the EM limitations impose a different behaviour at certain wheel-speeds. In order to maximize the regeneration, one should use as much brake torque as possible from the EM. It is possible to maximize the usage of the EM, however, increasing the usage of EM brake torque, increased the oscillations observed in the ABS request, which at the moment is inexplicable. Maximizing the usage of the EM, especially at the rear axle, may cause heavier oscillations and cause instability, since the wheels are more likely to start to slip. The main objective is to determine the optimal amount brake torque that should be used from the EM.

4.2.2 Comparison of slip when using brake blending and when not using brake blending

Figure 4.2.3 shows the slip of the front left wheel. The slip is only analyzed on the front left wheel for the same reasons as for the Approach II, where maximal usage of the EM brake torque was applied. For both Test Case 1 and 2 some bigger oscillations can be detected in the slip during brake blending. These oscillations may explain why the total torque during brake blending oscillates more than the total torque when only braking with friction brakes. Otherwise, overall the slip during brake blending (according to Approach III) and no brake blending (Approach I) is nearly identical.

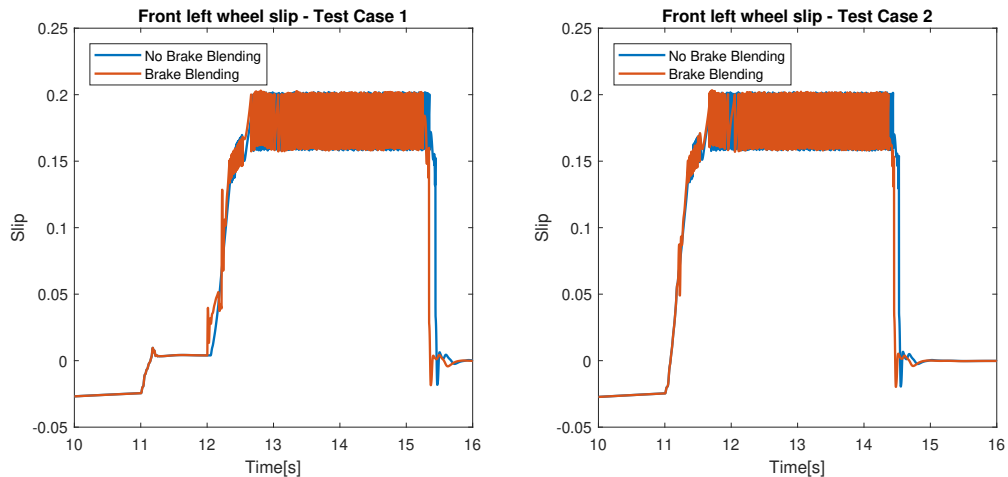


Figure 4.2.3: A visual representation of the slip comparison between Approach I and Approach III, for Test Case 1 (left plot) and Test Case 2 (right plot). Both plots are a representation of the front left wheel. The brake application ends at approximately 15.5s for Test Case 1 and around 14.5s for Test Case 2.

4.2.3 Comparison of deceleration when using brake blending and when not using brake blending

In Figure 4.2.4 the acceleration and deceleration is visualised for the entire cycle. The acceleration is nearly identical for the two presented cases, however the deceleration is different. More aggressive oscillations can be observed for deceleration during brake blending in both test cases. These oscillations are due to the oscillations in the total brake torque during brake blending. As mentioned earlier for Approach II, it can be observed that the deceleration is higher during braking, when brake blending (Approach III) is used compared to no brake blending (Approach I). It can also be seen from Test Case 1 that the EM at the start of braking provides with an earlier deceleration compared to no blending. This is because the EM has a faster response time compared to friction brakes. The specific details of this phenomena will not be investigated within this work, however, to utilize the potential of the EM response time, a deeper analysis is needed.

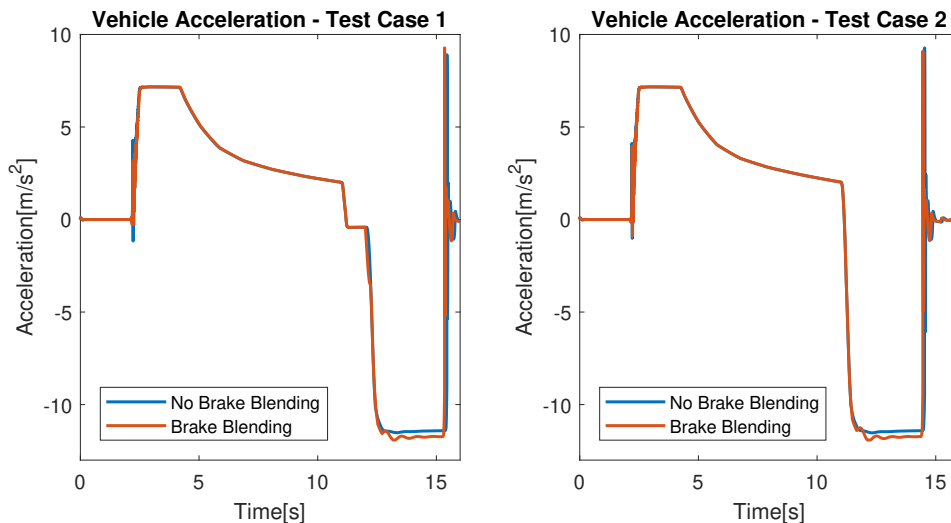


Figure 4.2.4: The figure is a representation of the resulting vehicle deceleration comparison, between Approach I and Approach III, during Test Case 1 (left plot) and Test Case 2 (right plot). The vehicle does not start to accelerate (positive valued curve) until $t \geq 2$ s for Test Case 1 and 2. For Test Case 1 the one second pause interval is starts at $t \approx 11$ s and ends at $t \approx 12$ s, when the pause interval is completed the brake application starts at time $t \geq 12$ s. In Test Case 2 the brake application is initiated at $t \geq 11$ s. For both Test Case 1 and 2 a positive spike at 1g-force is visible at around 15 s, meaning that the brake application is terminated and the vehicle is no longer in motion (this is not relevant and thus not considered in the results).

4.2.4 Comparison of velocity when using brake blending and when not using brake blending

For Approach III it can be seen in Figure 4.2.5 that the difference in vehicle velocity between blending and no blending, for Test Case 1, differs approximately by 0.1 m/s.

While Test Case 2 has the same vehicle velocity during blending and no blending. As in Approach II, this difference in velocity is negligible since it will not affect the brake distance remarkably.

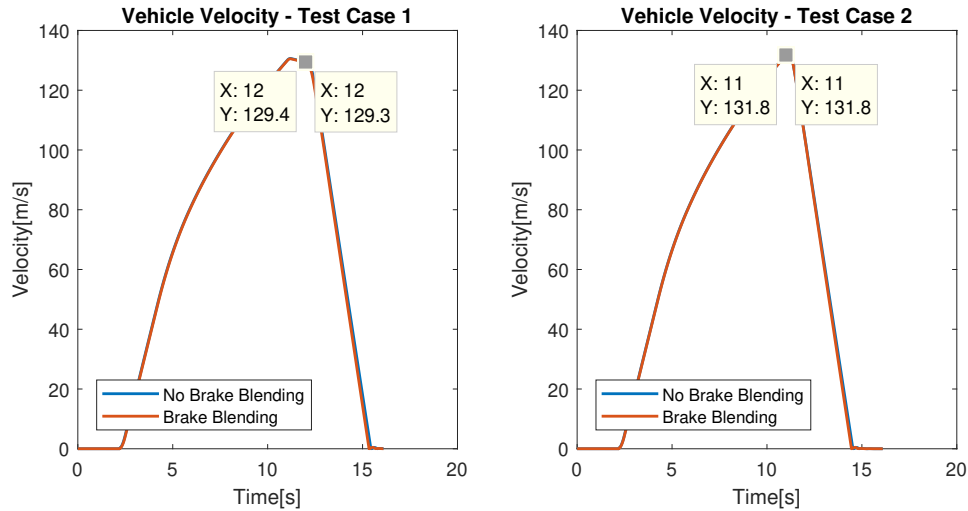


Figure 4.2.5: The figure is a representation of the resulting vehicle velocity when using Approach I and III, during Test Case 1 (left plot) and Test Case 2 (right plot). The vehicle does not start to accelerate until $t \geq 2$ s for Test Case 1 and 2. For Test Case 1 the one second pause interval starts at $t \approx 11$ s and ends at $t \approx 12$ s, when the pause interval is completed the brake applications starts at time $t \geq 12$ s. In Test Case 2 the brake application is initiated at $t \geq 11$ s. The brake application initiation is marked in both plots with a grey square, where it can be seen that velocity between Approach I and III differs for both cases.

4.2.5 Comparing brake distance when using brake blending and when not using brake blending

In Figure 4.2.6 it can be seen that the brake distance decreases about $2.1m$ in Test Case 1 and about $1.2m$ in Test Case 2. The decrease in distance is due to several reasons. One reason is that the total brake torque in the rear axle during brake blending is higher than when only braking with friction brakes. Another reason is that when brake blending is used for Test Case 1, the braking procedure is initiated earlier because of the instantaneous brake response from the EM. Thus, yielding a greater brake distance improvement compared to Test Case 2. One of the main reasons that the distance is decreased is due to how the ABS controller is modeled, meaning that a better ABS model could further improve the results.

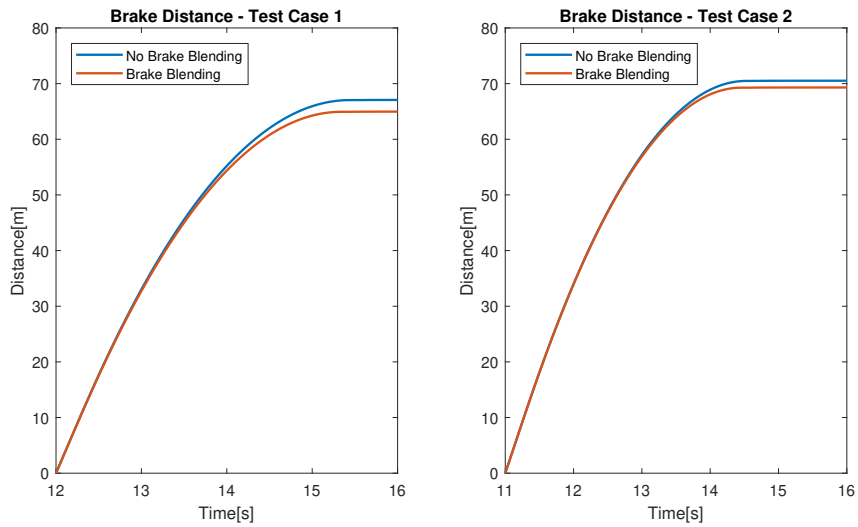


Figure 4.2.6: The figure is a representation of the resulting vehicle braking distance when using Approach I and III, during Test Case 1 (left plot) and Test Case 2 (right plot). The brake application starts at time $t \geq 12$ s for Test Case 1. In Test Case 2 the brake application is initiated at $t \geq 11$ s.

Figure 4.2.7 gives a clearer visualization of the brake distance reduction.

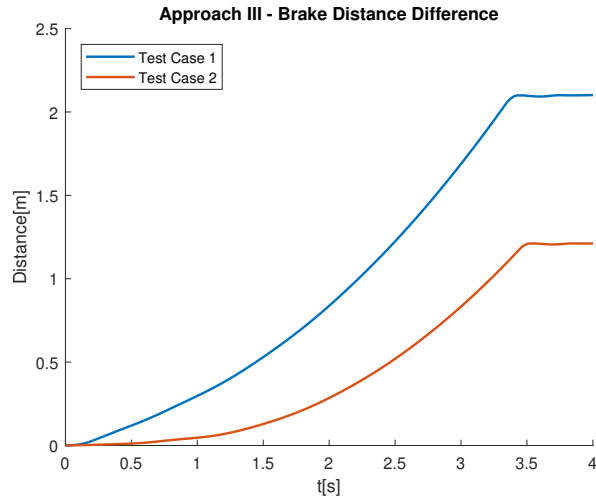


Figure 4.2.7: The figure is a representation of the brake distance difference between Approach I and Approach III for Test Case 1 and 2. The x-axis represents the time that the car is braking and the y-axis represents how big the difference is between the brake distance for Approach I and Approach III.

4.3 Design of experiments

In this section a design of experiments (DOE) setup is presented, this can be seen in Figure 4.3.1. DOE is a method to determine the correlation between input and output variables. This correlation is needed to understand the significance of certain parameters and how they should be controlled in order to receive optimal outputs. The three input parameters that have been analysed in this DOE are the road friction coefficient, velocity and the presence of a time gap prior to deceleration. The analyzed road friction coefficients are 0.5(Low(-)) and 1.0(High(+)) and the velocities are 100 km/h(Low(-)) and 130 km/h(High(+)). The pause in the DOE represents the time gap between accelerating and braking, this was either 0 seconds(Low(-)) or 1 seconds(High(+)).

	Velocity	Road fric.	Paus	Approach I Brake Distanc [m]	Approach II	Approach III
1	-	-	-	74.9	78.0	74.7
2	-	-	+	74.2	77.8	73.1
3	-	+	-	42.4	41.6	41.6
4	-	+	+	42.0	41.5	40.6
5	+	-	-	122.9	127.7	122.4
6	+	-	+	122.0	127.1	120.6
7	+	+	-	68.1	67.0	66.7
8	+	+	+	67.6	66.9	65.6

Figure 4.3.1: The figure represents a DOE where the different brake distance results for each Approach is visible.

The results in Table 4.3.1 show the different approaches adaptability to changing variables. It is observed from the results that Approach III gives the best results in all of the eight simulations performed, while Approach II gives the poorest results when a low road friction coefficient is applied. Approach II performs poorly on a low road friction coefficient value since the EM is handling all of the braking by itself, meaning that it needs to handle the pulsations as well. This is because a lower brake torque request from the ABS-soft will be sent directly to the EM, meaning that the EM will send the same amount of brake torque into the distribution and removing the portion otherwise sent to the frictional brake system. Figures 4.3.2 and 4.3.3, visualize the difference between Approach II and III regarding brake torque distribution for a road friction coefficient value of 0.5.

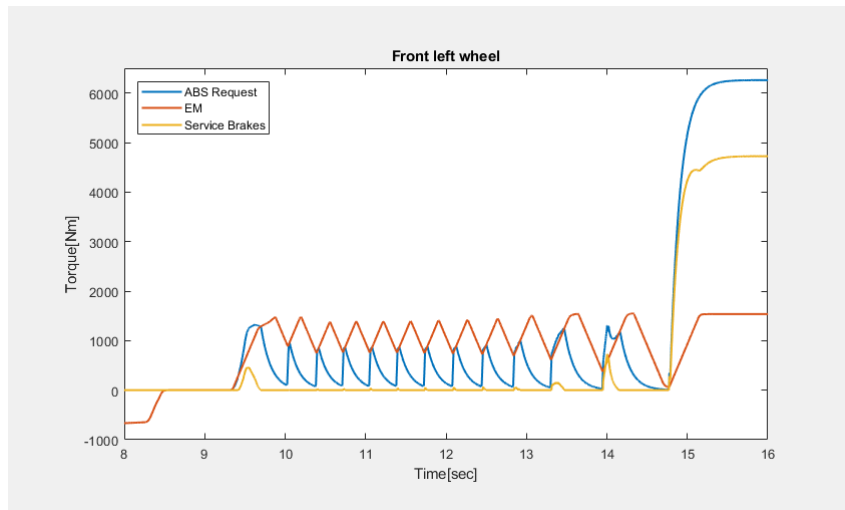


Figure 4.3.2: The Figure represents what happens with one of the wheels when Approach II performs poorly on a road friction coefficient of 0.5. It can be seen from the red EM curve how the electric motor is trying to pulsate but has a slow ramp-up, since the ramp-up time is limited by a comfort constraint.

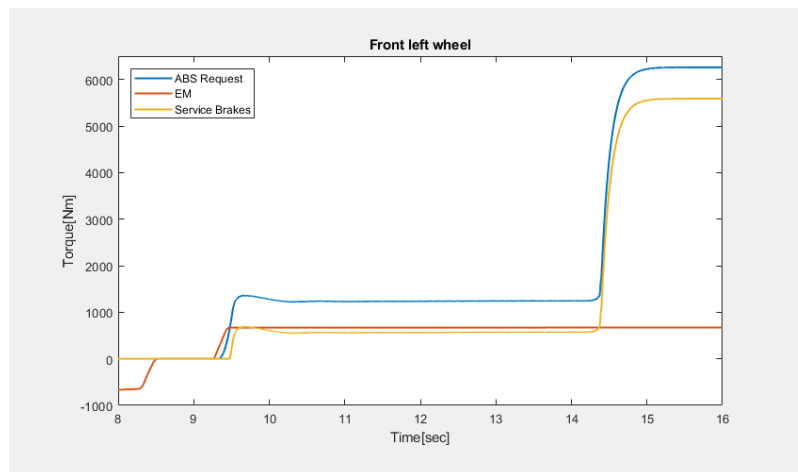


Figure 4.3.3: The Figure represents what happens with one of the wheels when Approach III performs well on low road friction coefficient. It can be observed that the pulsations are handled by the friction brakes and not by the EM as they are in Approach II.

5

Conclusion

The aim of this work was to construct a control model, that integrates a frictional brake system with a regenerative brake system during a ABS intervention. In order to achieve a desired brake torque distribution, two methods were developed. The overall main conclusion is that for both of these developed methods (referred to as Approach II and III in this report) an improved brake torque distribution was obtained and thereby a decrease in the brake distance compared to only using friction brakes (referred to as Approach I in this report). The following conclusions were additionally drawn:

- It was observed in the results that the torque request from the ABS controller oscillates and is higher if brake blending is implemented. This observation may be the reason to the decrease in the braking distance. Additionally, due to its shorter response time the EM reacts quicker, meaning that the car starts to brake sooner than when there is no brake blending. The two factors; response time and increased/oscillating brake torque have not been isolated and studied individually, thus the affect on brake distance for each parameter was not quantified in detail.
- Approach III, in which a look-up table was used to determine the EM brake torque request, has proven to be a very simple but effective method. This approach has its limitations in terms of adapting to new conditions that affect the ABS model input parameter values. Each element in the array of EM brake torque requests is dependent on the ABS torque request. If a new ABS model is implemented, one will need to use the extreme value function to calculate new EM brake torque requests, using the ABS request. Meaning, that the array of EM brake torque requests in the lookup table will have to be updated if a completely new ABS model other than ABS-soft, is implemented.
- Except from the decrease in brake distance, kinetic energy was converted into electric energy, which was fed to the battery. To meet the high sustainability demands, the goal is to recover as much electrical energy as possible. The results have shown that the EM can cover a significant amount of brake torque requests. Within this work it was determined to what level the EM torque could be utilized. Approach III used a lesser amount of EM brake torque than Approach II while managing to stop in a shorter distance. This means that always maximizing the usage of the EM can negatively affect the brake distance.

6

Recommendation for future work

Based on previous chapters, following items are recommended as a part of the future work:

- The lookup table, for Approach III, is currently using one input to decide which torque request it should output. This works well for a vehicle moving in a straight line, however, for braking scenarios that include turning and related stability issues, more analysis is needed. There are additional inputs to the lookup table, that may improve the torque distribution for a larger amount of driving scenarios, an example of such an input parameter may be steering angle, which is used to quantify torque request output during turning.
- This project has not considered any battery or temperature limitations. Meaning, that the effects coupled to these limitations are not known. Considering these limitations are thereby of importance since a robust model is required.
- From results it was concluded that the EM has a faster response time compared to the friction brakes. This implies that the EM can have a faster response to changes and thereby enabling the possibility to handle the pulsations from the ABS request better than the friction brakes. The current system was developed such that the friction brakes handled the pulsations requested by the ABS system and that the EM provided a constant brake torque. Since the EM responds quicker than friction brakes, it can be concluded that this process can be reversed, in which the EM would handle the pulsations instead which then could lead to a better slip-control and yield a shorter brake distance.
 - It may be possible to use a low and high pass filter to distribute the torque between friction brakes and the EM. Since the EM responds faster, the high frequencies of the torque signal should be handled by the EM and low frequencies by the friction brakes.
- In order to achieve better results, a more advanced ABS model is needed. The current ABS model is too simplistic and further development of this is required.
- The brake distance when using brake blending was decreased. An interesting topic for future work is to determine whether or not this reduction in brake distance is sufficient to consider regenerative braking during ABS intervention.
- Since all the results are only based on simulations in Simulink/CarMaker, more methods of validation are needed in order to be able to implement the controllers in a real vehicle. Thus, the following suggestion of further steps of model validation

6. Recommendation for future work

are: $\xrightarrow{\text{next}}$ HIL(Hardware in the loop) $\xrightarrow{\text{next}}$ Driving simulator $\xrightarrow{\text{next}}$ Boxcar $\xrightarrow{\text{next}}$ Brake dynamometer $\xrightarrow{\text{next}}$ Vehicle.

- Hardware in the loop (HIL) is a simulation tool used in order to test control systems. The plant is replaced with a simulation, which gives you the possibility to run tests that otherwise can damage a real plant.[19]
- Driving simulators substitutes actual driving with a artificial environment.[20]
- A boxcar is a vehicle which only consists of ECUs (electronic control units), sensors and wires with no body parts.[21]
- A brake dynamometer is used to measure the performance of a brake system and the different brake parts during diverse conditions.[22]

Bibliography

- [1] “Pure progressive performance.” [Online]. Available: <https://www.polestar.com/se/polestar-2/>
- [2] A. Mahmoudzadeh Andwari, A. Pesyridis, M.-B. Ricardo, and V. Esfahanian, “A review of battery electric vehicle technology and readiness levels,” *Renewable and Sustainable Energy Reviews*, vol. 78, pp. 414–430, 10 2017.
- [3] V. Vodovozov, A. Rassölkin, N. Lillo, and Z. Raud, “Energy saving estimates for regenerative braking and downhill driving of battery electric vehicles,” pp. 237–240, 10 2014.
- [4] A. Doyle and T. Muneer, *Traction energy and battery performance modelling*, 07 2017, pp. 93–124.
- [5] C. Lv, H. Wang, and D. Cao, “Chapter 8 - brake-blending control of evs,” in *Modeling, Dynamics and Control of Electrified Vehicles*, H. Zhang, D. Cao, and H. Du, Eds. Woodhead Publishing, 2018, pp. 275 – 308. [Online]. Available: <http://www.sciencedirect.com/science/article/pii/B9780128127865000082>
- [6] C. Lv, J. Zhang, Y. Li, and Y. Yuan, “Regenerative braking control algorithm for an electrified vehicle equipped with a by-wire brake system,” vol. 1, 04 2014.
- [7] S. A. Oleksowicz, K. J. Burnham, P. Barber, B. Toth-Antal, G. Waite, G. Hardwick, C. Harrington, and J. Chapman, “Investigation of regenerative and anti-lock braking interaction,” *International Journal of Automotive Technology*, vol. 14, no. 4, pp. 641–650, Aug 2013. [Online]. Available: <https://doi.org/10.1007/s12239-013-0069-0>
- [8] D. Meinel, T. Javied, S. Rast, C. Zipp, and J. Franke, “A multi-physics simulation approach for energy and cost analysis during the deceleration of high-speed trains,” *Procedia Manufacturing*, vol. 24, pp. 8–14, 01 2018.
- [9] S. Meitei, A. Kharghoria, U. Chetia, and S. Deka, “Regenerative braking along with abs system in hybrid vehicles,” 04 2016, pp. 317–320.
- [10] J. Shi, J. Wu, B. Zhu, Y. Zhao, W. Deng, and X. Chen, “Design of anti-lock braking system based on regenerative braking for distributed drive electric vehicle,” vol. 11, 04 2018.
- [11] M. Boerboom, “Electric vehicle blended braking maximizing energy recovery while maintaining vehicle stability and maneuverability.” 2012.

- [12] D. Peng, Y. Zhang, C. Yin, and J. Zhang, "Combined control of a regenerative braking and antilock braking system for hybrid electric vehicles," *International Journal of Automotive Technology*, vol. 9, pp. 749–757, 01 2008.
- [13] I. A. GmbH, "ipg-automotive.com," May 2020. [Online]. Available: <https://ipg-automotive.com/>
- [14] S. Rajendran, S. Spurgeon, G. Tsampardoukas, and R. Hampson, "Estimation of road frictional force and wheel slip for effective anti-lock braking system (abs) control," *International Journal of Robust and Nonlinear Control*, vol. 29, 10 2018.
- [15] C. Elmas, U. Guvenc, and M. DOGAN, "Tire-road friction coefficient estimation and experimental setup design of electric vehicle," *Balkan Journal of Electrical and Computer Engineering*, vol. 3, 12 2015.
- [16] M. Boerboom, "Electric vehicle blended braking maximizing energy recovery while maintaining vehicle stability and maneuverability." 2012.
- [17] E. Mohamed, S. Abouel-Seoud, and M. Elsayed, "Performance analysis of the abs control on parallel hybrid electric vehicle equipped with regenerative braking system," *SAE International Journal of Passenger Cars - Electronic and Electrical Systems*, vol. 8, pp. 477–491, 08 2015.
- [18] M. Burckhardt and R. Jornsens, "Fahrwerktechnik: Radschlupf-regelsysteme: Reifenverhalten, zeitablaufe, messung des drehzustands der rader, anti-blokier-system (abs), theorie hydraulikkreislaufe, antriebs-schlupf-regelung (asr), theorie hydraulikkreislaufe, elektronische regeleinheiten. leistungsgrenzen, ausgefuhrte anti-blockier-systeme und antriebsschlupf-regelungen," 1993.
- [19] "Matworks." [Online]. Available: <https://se.mathworks.com/help/physmod/simscape/ug/what-is-hardware-in-the-loop-simulation.html>
- [20] K.-H. Chang, "Chapter 8 - motion analysis," in *e-Design*, K.-H. Chang, Ed. Boston: Academic Press, 2015, pp. 391 – 462. [Online]. Available: <http://www.sciencedirect.com/science/article/pii/B9780123820389000089>
- [21] V. Bordyk, "Analysis of software and hardware configuration management for pre-production vehicles - a case study at volvo car corporation," 2012.
- [22] M. Kim, J. Kim, B. Goo, and N.-P. Kim, "Comparative studies of the tread brake dynamometer between dry and wet conditions," 10 2010, pp. 479–483.